NTNU

Norwegian University of
Science and Technology

Static Stiffness of Monopile Foundations Embedded in Nonhomogeneous Elastic Soil

Vasileios Tsalavrettas

Geotechnics and Geohazards
Submission date: July 2018
Supervisor: Gudmund Reidar Eiksund, IBM
Co-supervisor: Ana M. Page Risueno, IBM

Norwegian University of Science and Technology
Department of Civil and Environmental Engineering

NTNU – Trondheim
Norwegian University of
Science and Technology

Static Stiffness of Monopile Foundations Embedded in Nonhomogeneous Elastic Soil

Vasileios Tsalavrettas

Geotechnics and Geohazards

Submission Date: July 2018

Supervisors: Gudmund Reider Eiksund, IBM

Co-supervisor: Kristoffer Skjolden Skau, NGI

Department of Civil and Environmental Engineering
Norwegian University of Science and Technology (NTNU)

NORWEGIAN UNIVERSITY OF SCIENCE AND TECHNOLOGY
DEPARTMENT OF CIVIL AND ENVIRONMENTAL ENGINEERING

Report Title: **Static Stiffness of Monopile Foundations Embedded in Nonhomogeneous Elastic Soil**	Date: **24.07.2018** Number of pages: **95**	
	Master Thesis	X

Name: Vasileios Tsalavrettas

Professor in charge/supervisor: Gudmund Reidar Eiksund

Other external professional contacts/supervisors: Kristoffer Skjolden Skau

Abstract:
Monopiles are the main foundation type for offshore wind turbines. The number of wind farms around the world is increasing rapidly which leads to more demanding design methods. Until now the use of p-y curves was the main design method for pile foundations. These curves were established for long slender (flexible) piles with small diameter and length to diameter ratio $(L/D) > 35$, for the oil industry. Several studies for rigid piles are have also took place the last years. This leads to a need for studying the gap between these two different dimension situations (flexible and rigid), which is the major dimension for the monopiles.

For designing a methodology for calculating the deflection at the mudline the NGI's in-house program PILES was used. Therefore, a simulation with 3 different stiffness coefficients was held. These coefficients will be the K_F (lateral stiffness), K_M (rotational stiffness) and K_C (Coupling stiffness).

Firstly, a validation of the PILES results was essential to be conducted. So, a case study where the soil was considered as linear elastic with full saturated conditions, and the stiffness profile varies from constant elastic stiffness to linear and parabolic increase by depth. For the validation purpose the FEM program PLAXIS 3D was used. Also, well-established formulas from Gazetas and Shadlou represented the upper and lower boundaries of the study, for the flexible and rigid conditions respectively.

After proving the accuracy of the PILES program, a sensitive study took place. The results of this study were used to establish charts for calculating the stiffness coefficients. The results from the charts were compared to the program PILES and their accuracy is higher than 90%. Finally, an example of how to use the charts for calculating the stiffness coefficients were provided, as well as the deflections of the pile at the mudline level.

Keywords:

1. Monopile
2. Static stiffness
3. Elastic soil
4. Offshore foundations

_____

MASTER'S DEGREE THESIS

Spring 2018

Vasileios Tsalavrettas

Static Stiffness of Monopile Foundations Embedded in Nonhomogeneous Elastic Soil

BACKGROUND

The last decades the alarmingly high levels of CO_2 emissions are an issue that concerns more and more people. A cause that influences the climate change is the use of fossil fuel. One of the ways to reduce the harmful CO_2 footprint is to invest in renewable energy sources. The most common way to produce renewable energy is by wind turbines. Consequently, that led to a historical increase in the number of wind farms around the world.
The main foundation type of these offshore wind turbines is a large diameter single pile which is commonly referred to as monopile. That monopile is commonly used for water depths up to 30 meters. Its design is based on an open-ended pile with steel walls, which is embedded in the subsea soil, deep enough to prevent lateral movement and rotation.

TASK

The existing models are the industrial standard (i.e. p-y curves) which is an improved version of the former one from the 1970s, and two more recent approaches of the problem. The one of these new approaches is a closed form solution of the soil stiffness based on researches from Gazetas, Shadlou and Bhattacharya and others. The other one is based on the Finite Element Method. However, the drawback of the p-y curve method is the inaccurate results due to the uncoupled springs. For the closed form solutions is the limited range of application, there are solutions for slender piles and for rigid piles. As for the FEM programs is that they are time-consuming and specialists are required to operate. As a result, the new procedure that will be presented will include a wider range of application, ease in use and higher accuracy.

Task description

The main objective of the master thesis is:

- The development of a procedure for establishing the stiffness of monopiles. The stiffness should be described at seabed level and consider the rotational and horizontal stiffness components.

To obtain this main objective, the following secondary objectives must be obtained:

- Understand the mechanism of laterally piles, focusing on the DNV-GL codes based on the fundamental p-y curves
- Research for new approaches on the topic of laterally loaded piles
- Understand the background methodology of the NGI'S in-house program PILES
- Establish a validation method of the program PILES according to well-established methods

Professor in charge:

Professor Gudmund Reidar Eiksund

Department of Civil and Transport Engineering, NTNU
Date: 24.07.2017

_____
Professor in charge (signature)

PREFACE

This is a master's thesis in the Department of Civil and Environmental Engineering at the NTNU University as part of the MSc in Geotechnics and Geohazards. The work was carried out during the spring semester 2018 after a preliminary study at the fall semester 2017.

The idea for this project was brought up by the PhD student Ana M. Page Risueno at an information meeting at NGI Trondheim. The project is part of a larger research project from NGI and other companies, focusing on more effective design of offshore wind turbines.

Trondheim, 2018-06-24

Vasileios Tsalavrettas

ACKNOWLEDGMENT

First of all, I would like to thank Dr. Kristoffer Skjolden Skau for his guidance during the whole semester and spending time for this project even at his free time. Also, I would like to thank Prof. Gudmund Reider Eiksund for his help in situations of stress and using PLAXIS. Then the PhD student, soon Doctor, Ana M. Page Risueno for giving me this change to study such an interesting project. Finally, my classmates and friends which helped and supported me the difficult times of this semester.

V.T.

ABSTRACT

Monopiles are the main foundation type for offshore wind turbines. The number of wind farms around the world is increasing rapidly which leads to more demanding design methods. Until now the use of p-y curves was the main design method for pile foundations. These curves were established for long slender (flexible) piles with small diameter and length to diameter ratio (L/D) $>$ 35, for the oil industry. Several studies for rigid piles are have also took place the last years. This leads to a need for studying the gap between these two different dimension situations (flexible and rigid), which is the major dimension for the monopiles.

For designing a methodology for calculating the deflection at the mudline the NGI's in-house program PILES was used. Therefore, a simulation with 3 different stiffness coefficients was held. These coefficients will be the K_F (lateral stiffness), K_M (rotational stiffness) and K_C (Coupling stiffness).

Firstly, a validation of the PILES results was essential to be conducted. So, a case study where the soil was considered as linear elastic with full saturated conditions, and the stiffness profile varies from constant elastic stiffness to linear and parabolic increase by depth. For the validation purpose the FEM program PLAXIS 3D was used. Also, well-established formulas from Gazetas and Shadlou represented the upper and lower boundaries of the study, for the flexible and rigid conditions respectively.

After proving the accuracy of the PILES program, a sensitive study took place. The results of this study were used to establish charts for calculating the stiffness coefficients. The results from the charts were compared to the program PILES and their accuracy is higher than 90%. Finally, an example of how to use the charts for calculating the stiffness coefficients were provided, as well as the deflections of the pile at the mudline level.

CONTENTS

1 INTRODUCTION

1.1 BACKGROUND

The last decades the alarmingly high levels of CO_2 emissions are an issue that concerns more and more people. A cause that influences the climate change is the use of fossil fuel (IRENA, 2018). One of the ways to reduce the harmful CO_2 footprint is to invest in renewable energy sources. The most common way to produce renewable energy is by wind turbines (Europe, 2017). Consequently, that led to a historical increase in the number of wind farms around the world. Although the onshore wind farms have been used frequently until nowadays, the offshore farms tend to be a more frequent choice due to several factors. Some of them are the stronger and more constant offshore winds, which can produce more energy. Additionally, at offshore farms bigger and more efficient turbines can be used. Also, there will be no aesthetic problem with the local population, since the farms will not be visible from the mainland.

The main foundation type of these offshore wind turbines is a large diameter single pile which is commonly referred to as monopile. That monopile is commonly used for water depths up to 30 meters. Its design is based on an open-ended pile with steel walls, which is embedded in the subsea soil, deep enough to prevent lateral movement and rotation.

The way to predict the lateral movement and rotation of the pile is to calculate the interaction between the soil and the pile. The model to accomplish that was developed in the 1970s when the demand for offshore structures was increased. By that time the technology and knowledge of the offshore structure field were not fully developed. As a result, engineers and specialists in the field needed a more accurate model. The need of that new approach would not only be to increase the safety margin of the construction but also to reduce the cost of the construction. Also, that approach would be important considering that the cost of the foundation at an offshore monopile is almost 1/3 of the total cost of the whole structure. Consequently, an accurate approach is of huge benefit to the industry.

Currently, the existing models are the industrial standard (i.e. p-y curves) which is an improved version of the former one from the 1970s, and two more recent approaches of the problem. The one of these new

approaches is a closed form solution of the soil stiffness based on researches from Gazetas, Shadlou and Bhattacharya and others (Gazetas, 1984) (Shadlou & Bhattacharya, 2016). The other one is based on the Finite Element Method. However, the drawback of the p-y curve method is the inaccurate results due to the uncoupled springs. For the closed form solutions is the limited range of application, there are solutions for slender piles and for rigid piles. As for the FEM programs is that they are time-consuming and specialists are required to operate. As a result, the new procedure that will be presented will include a wider range of application, ease in use and higher accuracy.

1.2 OBJECTIVES

The main objective of the master thesis is:

- The development of a procedure for establishing the stiffness of monopiles. The stiffness should be described at seabed level and consider the rotational and horizontal stiffness components.

To obtain this main objective, the following secondary objectives must be obtained:

- Understand the mechanism of laterally piles, focusing on the DNV-GL codes based on the fundamental p-y curves
- Research for new approaches on the topic of laterally loaded piles
- Understand the background methodology of the NGI'S in-house program PILES
- Establish a validation method of the program PILES according to well-established methods

1.3 LIMITATIONS

- Only clay was used for the analysis at undrained conditions.
- Only undrained conditions have been considered.
- Only the length of the pile below the seabed was modelled, thus the weight of the structure above was ignored and only lateral force along the x axis and moment around the y axis were used.
- The soil was assumed to be linear elastic.
- All the materials considered isotropic.

- No effect from the pile installation to the surrounding soil was considered.
- Only for static analyses were carried out.
- The diameter and the wall thickness of the pile were kept constant.
- No gap between the pile and the soil at the seabed elevation was modelled.

2 THEORY AND PREVIOUS METHODS

2.1 PHYSICAL MECHANISM OF LATERALLY LOADED PILES

The offshore monopiles have a different response than the piles that are used for the oil industry, as it can be proved by Kallehave that the measured values of deflections are 20% higher than the DNV-GL recommendations by the p-y curves method (Dan Kallehave, Byrne, Thilsted, & Mikkelsen, 2015). Thus, the mechanism of lateral load transfer is the same for all piles so, a short introduction of the mechanism of the load transfer is needed before the analysis of this thesis.

2.1.1 Load transfer mechanisms of piles

Therefore, when a lateral load is applied on a pile, the forces are distributed on the soil around the pile by the soil's lateral resistance. This resistance is depending on the pile-soil relative stiffness and allows the pile to move by two major mechanisms, translation, and rotation.

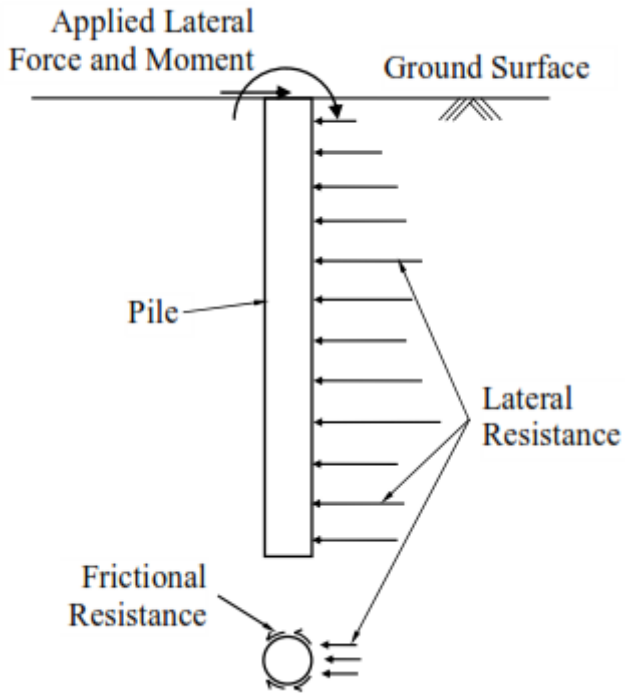

Figure 1: Major mechanisms of laterally loaded pile. From (Mukherjee & Dey, 2016)

The soil's resistance to the movement of the pile can be described with two main ways, the passive and the active. The first one is divided into the compressive stresses at the front of the pile, and the shear stresses at the sides. The active occurs when suction is developed at the back side of the pile. It may happen that a cavity between the pile and the soil at the rear side can be formed, which can lead to a situation where only the net soil pressure is applied on the area of the pile which the cavity has opened. It must be noted this scenario is not taken into account in this thesis because finite element methods are used for the calculations and are not capable of this kind of simulation. Concluding the external load comes to equilibrium with the soil resistance at the active length of the pile.

2.2 Design Criteria for Monopile Foundations

The main methods to design offshore wind turbines have been made by DNV-GL and API (Veritas, 2004) (API, 2011), and they are used worldwide as design codes for offshore foundations. Though recent studies which have been conducted by Kallehave (Dan Kallehave et al., 2015) and Hanssen (Hanssen, 2016), shows that these guidelines are not entirely accurate on calculating the soil behaviour. Consequently, the design tends to be more conservative, meaning that the structure is manufactured stiffer which subsequently makes it costlier. Thus, most of the construction companies are investing in projects which can find ways to calculate the exactly needed stiffness of the structures and make the whole construction more efficient and reduce the cost.

2.2.1 Ultimate Limit State

Based on the codes from DNV-GL (Veritas, 2004), for calculating the ultimate limit state (ULS) of a structure, the design soil strength and the design loads must be used. According to Eurocode 7 these design values are calculated by the characteristic values by using the material factor. For soils by dividing with the material factors and for loads by multiplying the characteristic values with the material factors.

$$R_d = \frac{R_k}{\gamma} \;\; and \;\; F_d = F_k\,\gamma \tag{2.4}$$

Where

- $R = soil\ resistance$
- $F = load$
- $d = design$
- $k = characteristic$
- $\gamma = material\ factor$

By that way, the ultimate capacity of the soil and the structure is calculated. For the monopiles, the situation is different when the design is based on the lateral resistance and not the vertical. Therefore, the p-y curves method is proposed, which is based on the beam on foundation approach. Although the p-y curve method is mostly used for long piles with small diameter (slender), the offshore monopiles foundations have larger diameters, so designing with the same method can be used but only with special considerations, according to DNV-GL (Veritas, 2004) codes.

While designing a monopile foundation, the common procedure is checking for the ultimate capacity with a combination of lateral loading and moment loading. The monopile capacity is formed by the lateral pile resistance and to verify the acceptable pile capacity, the following requirements must be fulfilled:

1) The total theoretical design lateral pile resistance must be greater than the design lateral load, force and moment, which is applied at the pile head.
2) The lateral displacement at the pile head must not exceed some specified limit. The lateral displacement must be calculated for the design lateral load and moment in combination with characteristic values of the soil resistance and soil stiffness.

2.3 ANALYSES METHODOLOGY

There are three fundamental methods of approaching the analysis of the soil-pile response on lateral loads. The first one is the *Beam on Foundation* which was initially introduced by Winkler (Winkler, 1867) and the more recent is the *Continuum Approach*. Finally closed form

solutions for slender (Gazetas, 1984) and rigid (Shadlou & Bhattacharya, 2016) piles will be presented.

2.3.1 Winkler Beam of Foundation & p-y Springs

The first attempt to understand and establish was made by Emil Winkler (Winkler, 1867) in 1867. The idea was that simple springs responses can express the soil deflection. Later with the research of Biot (Biot, 1922) first and Hetényi's after (Hetenyi, 1946) the finalized approach presented. So, the pile is modelled as several consecutive beam-column elements, supported by nonlinear springs applied at the nodal points between the elements. This approach can be solved with a closed form solution from Euler-Bernoulli beam on elastic foundation.

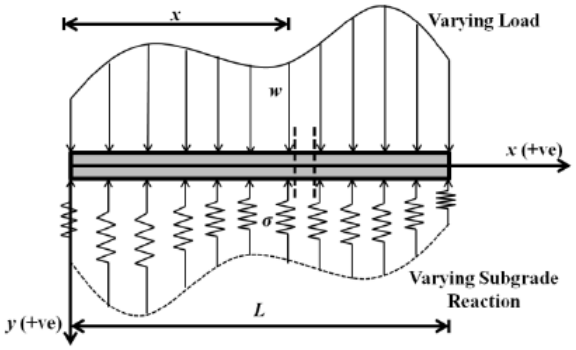

Figure 2: Display of the Winkler's Beam on Foundation approach. From (Mukherjee & Dey, 2016)

The equation for the Euler-Bernoulli beam for an elastic solution with general pile bending stiffness EI, which is applied to the Beam on Foundation Approach is presented in a fourth order differential equation:

$$EI\frac{d^4y}{dz^4} + Q_A\frac{d^2y}{dz^2} - p(y) + q = 0 \tag{2.1}$$

with

$$EI\frac{d^3y}{dz^3} + Q_A\frac{dy}{dz} = Q_L \tag{2.2}$$

and

$$EI\frac{d^2y}{dz^2} = M \tag{2.3}$$

where:

- $z = position\ in\ depth\ along\ the\ pile$
- $y = lateral\ displacement\ of\ the\ pile$
- $EI = bending\ stiffness\ of\ the\ pile$
- $Q_A = the\ axial\ force\ on\ the\ pile$
- $Q_L = the\ lateral\ force\ on\ the\ pile$
- $p(y) = the\ lateral\ soil\ reaction$
- $q = a\ distributed\ load\ along\ the\ pile$
- $M = the\ bending\ momenton\ the\ pile$

Closed form solutions, as the one above, are easy and quick to use but there is an important assumption which must be taken into account, and this is that the soil behaves only as a linear and homogeneous medium. Though in reality, the soil is mostly a non-linear and non-homogeneous medium. So, the equation (2.1) must be solved, with a finite difference method (Basu, Salgado, & Prezzi, 2008) to end up with a solution. Solving this approach lead to the p-y curves method which will be analysed in more details later in this thesis.

According to the previous subchapter, the recommendations from API and DNV-GL for calculating the ultimate limit state (ULS) is based on the p-y curve method. Thus, here a short introduction will take place to understand the main mechanism of this method and the main differences with the method that is proposed in this thesis.

Firstly, the p-y curve method was established for flexible piles which are used in the oil industry. So, this method has a major disadvantage in predicting the behaviour of piles with a bigger diameter.

Another difference approach of the p-y method is that it is focusing on the resistance along the whole length of the pile and not on the pile head at the mudline level. Furthermore, if one takes a close look at the formulas proposed by Matlock for soft clays, Reese for stiff clays, and Reese and O'Neil for sands, the calculations of the ultimate resistance have no correlation with the properties of the pile apart from the

diameter (Matlock, 1970) (Reese, Cox, & Koop, 1975) (O'Neill & Murchison, 1983).

$$p_u = N_p \, s_u \, D \tag{2.5}$$

$$p_u = (C_1 \, z + C_2 \, D) \, \gamma' z \tag{2.6}$$

$$p_u = C_3 \, D \, \gamma' z \tag{2.7}$$

Where

- $p_u = ultimate\ resistnace\ [kPa]$
- $N_p = nondimensioanl\ ultimate\ resistance\ coefficient$
- $s_u = soil\ shear\ strength\ [kPa]$
- $D = pile\ diameter\ [m]$
- $\gamma' = effective\ soil\ unit\ weight\ [kN/m^3]$
- $z = depth\ from\ seafloor\ [m]$
- $C_i = coefficients\ determined\ as\ a\ function\ of\ \varphi'$

The equation (2.5) is used for both soft and stiff clays, but the resistance coefficient N_p has different values. As for the equations (2.6) and (2.7) are for calculating the ultimate resistance in swallow and deep depth in respect.

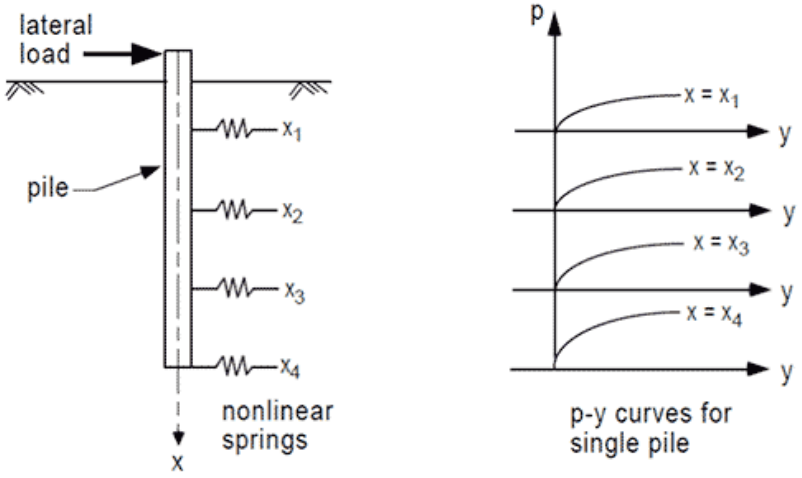

Figure 3: Uncoupled springs along the pile for p-y curve method

Finally, one of the most important disadvantages of the p-y curve method in calculating the deflections is that the fundamental way of calculating is based on the Winkler's method (Winkler, 1867). As it was mentioned at the beginning of the chapter, this method is simulating uncoupled springs along the pile.

This way the effect from each spring is only for specific depth without considering the resistance of the whole system pile/soil. Thus, the total deflections on the pile head will not be an accurate representation of the total interaction of the pile when is laterally loaded.

2.3.2 Continuum Approach

This method is considered to be more accurate comparing the previous one and that is because here the soil is treated as a three-dimension continuum. But even at this method the assumption that the soil is a collection of different particles which is enough homogeneous to be considered as the same material. The way this method works is by dividing the soil into elements which interact with the neighbouring elements. That way different type of soil structures can be modelled and analysed considering the coupling effects between them.

Several researchers have proposed analytical solutions for this method, one of the first was Baguelin et al. (Baguelin, Frank, & Said, 1977) with a discoid shape plane strain analysis in an elastic medium around the pile. Another more recent one is from Gupta and Basu (Gupta & Basu, 2016) where they proposed a three-dimension solution which in an elastic medium. Though the most common and widely used application of this method is the Finite Element, which nowadays is considered to be the most efficient and accurate tool for geotechnical engineers. Although the FE method has some disadvantages, which mostly has to do with time-demanding design of the model and the analysis of it, especially when high resolution is expected.

2.3.3 Closed Form Solutions

As it was mentioned before, in the offshore industry traditionally the p-y method was used to calculate the ultimate resistance of the pile when it is laterally loaded. After that, the deflection and rotation of the pile head at the mudline, along with stiffness of the foundation system, can be calculated. This method was analysed before based on the DNV-GL codes (Veritas, 2004). In addition, it has predicted from Kallehave that

there are major inaccuracies in the prediction of the foundation stiffness (D Kallehave, Thilsted, & Liingaard, 2012). Thus, many researchers have recently worked on developing design methodologies for the large diameter monopiles with ratio length to diameter typically in the range between 4-10. A new finite element analysis approach has been presented in Zdravkovic (Zdravković et al., 2015), and a new design method has been proposed by Byrne et al (Byrne et al., 2015a). Field testing has also been carried out to improve understanding of Byrne et al (Byrne et al., 2015b).

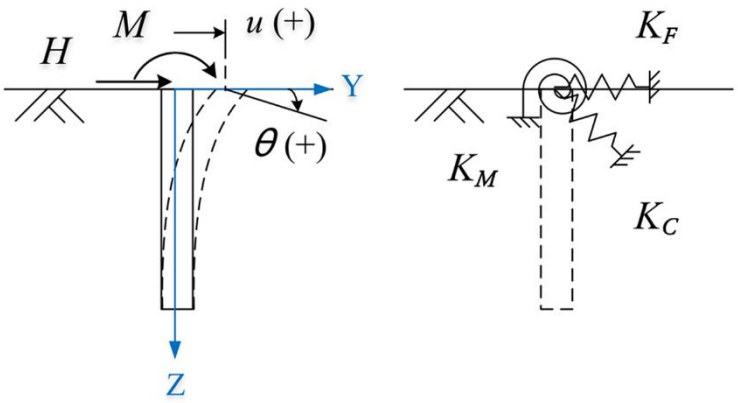

Figure 4: Coupled springs at the pile-head

The method which is going to be analysed in this thesis is based on the continuum approach. A simplified outline of this model can be modelled with three springs to calculate directly the foundation's stiffness. These three springs are simulating the horizontal stiffness K_F, the rotational stiffness for moment around a horizontal axis K_M, and the coupling stiffness which develop between the lateral load and the rotation around the horizontal axis K_C. This approach is based on the work of several researchers such as (Zaaijer, 2006), (Adhikari & Bhattacharya, 2011), (Adhikari & Bhattacharya, 2012), (Lombardi, Bhattacharya, & Wood, 2013), (Zania, 2014), (Damgaard, Zania, Andersen, & Ibsen, 2014), (Arany, Bhattacharya, Adhikari, Hogan, & Macdonald, 2015), (Abed, Bouzid, Bhattacharya, & Aissa, 2016).

To calculate these stiffness coefficients the following parameters are needed.

- $D = Diameter\ of\ the\ pile$
- $L = Length\ of\ the\ pile$
- $Ground\ profile\ (constant, linear\ or\ parabolic)$
- $E_{ref} = Elasticity\ modulus\ at\ the\ depth\ of\ one\ pile\ diameter$
- $E_p = Elasticity\ modulus\ of\ the\ pile$

The separation of the pile behaviour as flexible or rigid has to do with the total length of the pile compared to the active length of the pile. This active length is the upper part which experiences the displacement during the lateral loading. So, piles which are longer than the active length and have the same diameter behave identically. According to Gazetas for different type of soil profile the calculation is based on the following formulas (Gazetas, 1991):

$$l_c = 2\,D\left(\frac{E_p}{E_{ref}}\right)^{0.25} \quad for\ constant\ soil\ modulus \tag{2.8}$$

$$l_c = 2\,D\left(\frac{E_p}{E_{ref}}\right)^{0.20} \quad for\ linear\ soil\ modulus \tag{2.9}$$

$$l_c = 2\,D\left(\frac{E_p}{E_{ref}}\right)^{0.22} \quad for\ parabolic\ soil\ modulus \tag{2.10}$$

Also, according to the elastic continuum approach proposed by Randolph (Randolph, 1981), the active length of the pile can be expressed through the modified shear modulus G^* of the soil and the equivalent Young's modulus of the pile E_{eq}. With this, the active pile's length is calculated as:

$$l_c = D\left(\frac{E_{eq}}{G^*}\right)^{0.29} \tag{2.11}$$

Where

- $E_{eq} = \frac{(EI)_p}{\left(\frac{D^4 \pi}{64}\right)}$
- $G^* = \bar{G}\left(1 + \frac{3}{4}\nu\right)$
    - $\bar{G} = Average\ shear\ modulus\ along\ the\ pile\ length$
    - $\nu = Poisson'sratio$

Analytical solutions are seldom available for a general subgrade reaction approach, however, simplified expressions are applicable for slender and rigid piles by Poulos and Davis (Poulos & Davis, 1980). Then several different approaches have been developed to correlate horizontal (F_h) and bending moment (M) loads with the pile head displacement (u) and the rotation (θ). These expressions can be easily transformed into a stiffness matrix form of the load response in terms of the three springs (K_F, K_M and K_C). Apart from this method which was initially proposed by Poulos and Davis, many more researchers approached this topic. Some of the most significant are Gazetas which developed similar expressions for slender piles (Gazetas, 1984) also his method is also part of the Eurocode 8 Part 5 (European Committee for Standardization 2003),Randolph developed similar method for slender piles in both homogeneous and linear inhomogeneous soils (Randolph, 1981), Pender developed for slender piles (Pender, 1993), Shadlou and Bhattacharya for both slender and rigid piles (Shadlou & Bhattacharya, 2016) and again from Poulos and Davis following Barber proposed formulas for both slender and rigid piles from (Poulos & Davis, 1980) (Barber, 1953).

2.3.4 Flexible (Slender)

Flexible piles have been a study case for several years due to the correlation with the oil industry. Consequently, several researches tried to carry out sufficient calculations for the stiffness. The most well known and also the one that is used at the Eurocode 8, is the one from Gazetas (Gazetas, 1984). The formulas for different spring and soil profile are presented below:

For homogeneous soil

$$K_F = 1{,}08D\,E_{ref}\left(\frac{E_p^*}{E_{ref}}\right)^{0{,}21} \quad K_M = 0{,}16D^3\,E_{ref}\left(\frac{E_p^*}{E_{ref}}\right)^{0{,}75} \quad K_C = -0{,}22D^2\,E_{ref}\left(\frac{E_p^*}{E_{ref}}\right)^{0{,}5}$$

For linear inhomogeneous soil

$$K_F = 0{,}6D\,E_{ref}\left(\frac{E_p^*}{E_{ref}}\right)^{0{,}35} \quad K_M = 0{,}14D^3\,E_{ref}\left(\frac{E_p^*}{E_{ref}}\right)^{0{,}8} \quad K_C = -0{,}17D^2\,E_{ref}\left(\frac{E_p^*}{E_{ref}}\right)^{0{,}6}$$

For parabolic inhomogeneous soil

$$K_F = 0{,}79D\,E_{ref}\left(\frac{E_p^*}{E_{ref}}\right)^{0{,}28} \quad K_M = 0{,}15D^3\,E_{ref}\left(\frac{E_p^*}{E_{ref}}\right)^{0{,}77} \quad K_C = -0{,}24D^2\,E_{ref}\left(\frac{E_p^*}{E_{ref}}\right)^{0{,}53}$$

Where $E_p^* = E_p\left(1 - \left(\frac{r-t}{r}\right)^4\right)$

2.3.5 Rigid

Rigid piles have not been a subject of studying as extensive as flexible piles. So, over the years the most complete study of rigid piles with different soil profiles was made by Shadlou and Bhattacharya (Shadlou & Bhattacharya, 2016). This study includes the following formulas for different spring and soil profile to calculate the stiffness coefficients:

For homogeneous soil

$$K_F = \frac{3{,}2\,E_{ref}\,D}{1+|\nu-0{,}25|}\left(\frac{L}{D}\right)^{0{,}62} \quad K_M = \frac{1{,}65\,E_{ref}\,D^3}{1+|\nu-0{,}25|}\left(\frac{L}{D}\right)^{2{,}5} \quad K_C = -\frac{1{,}7\,E_{ref}\,D^2}{1+|\nu-0{,}25|}\left(\frac{L}{D}\right)^{1{,}56}$$

For linear inhomogeneous soil

$$K_F = \frac{2{,}35\,E_{ref}\,D}{1+|\nu-0{,}25|}\left(\frac{L}{D}\right)^{1{,}53} \quad K_M = \frac{1{,}58\,E_{ref}\,D^3}{1+|\nu-0{,}25|}\left(\frac{L}{D}\right)^{3{,}45} \quad K_C = -\frac{1{,}77\,E_{ref}\,D^2}{1+|\nu-0{,}25|}\left(\frac{L}{D}\right)^{2{,}5}$$

For parabolic inhomogeneous soil

$$K_F = \frac{2{,}66\,E_{ref}\,D}{1+|\nu-0{,}25|}\left(\frac{L}{D}\right)^{1{,}07} \quad K_M = \frac{1{,}63\,E_{ref}\,D^3}{1+|\nu-0{,}25|}\left(\frac{L}{D}\right)^{3} \quad K_C = -\frac{1{,}8\,E_{ref}\,D^2}{1+|\nu-0{,}25|}\left(\frac{L}{D}\right)^{2}$$

The stiffness expressions for slender and rigid piles can be easily converted to a stiffness matrix based on a three-spring model

$$\begin{bmatrix} F \\ M \end{bmatrix} = \begin{bmatrix} K_F & K_C \\ K_C & K_M \end{bmatrix} \begin{bmatrix} u \\ \theta \end{bmatrix} \tag{2.12}$$

Where

- $F = The\ lateral\ force\ on\ the\ pile$
- $M = The\ bending\ Moment\ on\ the\ pile$
- $u = The\ lateral\ displacement\ on\ the\ mudline$
- $\theta = The\ inclination\ from\ the\ initial\ state\ of\ the\ pile$

For the calculation of the lateral displacement (u) and inclination (θ) a reference point is needed. The easiest way is to choose the centreline of the pile at the mudline level. Then the elastic stiffness of the system is expressed by the three dimensionless stiffness coefficients, (K_F) for the horizontal stiffness, (K_M) for the rotational stiffness for moment around a horizontal axis, and (K_C) for the coupling stiffness which develop between the lateral load and the rotation around the horizontal axis. The deformations (displacement and inclination) can be calculated by using the matrix from above. These expressions can be seen below:

$$u = \frac{K_M}{K_F\, K_M - K_C^2} F - \frac{K_C}{K_F\, K_M - K_C^2} M \tag{2.13}$$

$$\theta = \frac{K_F}{K_F\, K_M - K_C^2} M - \frac{K_C}{K_F\, K_M - K_C^2} F \tag{2.14}$$

2.3.6 Caissons

Another approach for an offshore foundation, similar to rigid piles, are the caisson foundations. Caissons can be described as very short piles with a ratio of length to diameter smaller than 2. A sensitivity study on this type of foundation with a similar approach with the present thesis was made by Doherty. Doherty's study (J. Doherty, Houlsby, & Deeks, 2005) the same soil profiles with this thesis were used, with more details on that topic in the following chapter 4. Furthermore, the study took place for two horizontal directions with moment around these directions, and for the vertical direction and torsion around it.

The modelling for that project was based on a scaled boundary finite element method. This method was firstly proposed by Wolf and Song and it is a fusion of the typical finite element and the boundary element method (Wolf & Song, 1996). Then after several additions the final form, of which was used, was presented by Doherty and Deeks (J. P. Doherty & Deeks, 2003). By using the cylindrical coordinate system and Fourier series to analyse the matrixes which give the displacement, this method comes up with a global stiffness matrix. This matrix can be used with a linear equation of the form:

$$\{P_n\} = [K_n]\,\{u_n\} \tag{2.15}$$

Where

- $\{P_n\} = vector\ of\ nodal\ forces$
- $[K_n] = stiffness\ matrix$
- $\{u_n\} = vector\ of\ nodal\ displacement$

One of the major influences from Doherty's study to the present thesis is about the establishment of a dimensionless parameter J in order to normalize the results. For the case study of the caisson, it was made proportional to the thickness (t) of the caisson. Therefore, this expression is:

$$J = \frac{E_s\, t}{G_R\, R} \tag{2.16}$$

Where

- $E_s = Young's\ modulus\ of\ the\ caisson$
- $G_R = specific\ shear\ modulus\ at\ depth\ of\ one\ ratio$
- $R = ratio\ of\ the\ caisson$
- $t = thickness\ of\ the\ caisson's\ wall$

Then it was shown that from that coefficient J and by using the scaled boundary finite element method, some graphs can be generated which are displaying unique values of each one of the stiffness coefficients. Then for calculating accurate and fast the J coefficient, the following formula was developed:

$$K(J) = \frac{K_0 + (J/J_m)^p \, K_\infty}{1 + (J/J_m)^p} \tag{2.17}$$

Where

- $K_0 = value\ of\ stiffness\ coefficient\ when\ J\ approaches\ 0$
- $K_\infty = value\ of\ stiffness\ coefficient\ when\ J\ approaches\ \infty$
- $J_m = value\ of\ J\ at\ K = (K_0 + K_\infty)/2$
- $p = proportional\ to\ the\ gradient\ of\ the\ curve\ at\ J_m$

In this paper from Doherty, there are listed tables with values of the above parameter for different soil condition in order to calculate the correct stiffness coefficient and then calculate the deflections at the top of the caisson (J. Doherty et al., 2005).

3 RESEARCH METHOD

3.1 PILES PROGRAM

The purpose of using the PILES program (Kaynia & Kausel, 1991) is the computational effectiveness. The program was originally developed for analyses of dynamic and seismic response of piles or group of piles but can also be used for static problems. The program describes piles in a semi-infinite soil medium. Though at this thesis only the static response on a single pile will be applied.

The program model is based on a pile embedded in a viscoelastic soil medium which is located on top of a half space. The soil medium can be separated in layers where each one of these, along with the half space, can be described by the Young's modulus (E_s), density (ρ_s), shear wave velocity (v_s), Poisson's ratio (v_s) and the hysteric damping ratio (β_s). The pile is assumed as a linear elastic material with Young's modulus (E_p), density (ρ_p), Poisson's ratio (v_p), diameter (D) and length (L). One of the limitations is the assumption of the lack of gap development between the pile and soil.

To be able to model the pile/soil interaction the pile must be discretised to ℓ arbitrary cylindrical pieces along the pile shaft and one piece at the tip of the pile. Each one of the pieces is identified by a node at the centre of its piece and has a constant value of traction. All the values create a piecewise distribution which simulates the actual distribution of traction on the pile.

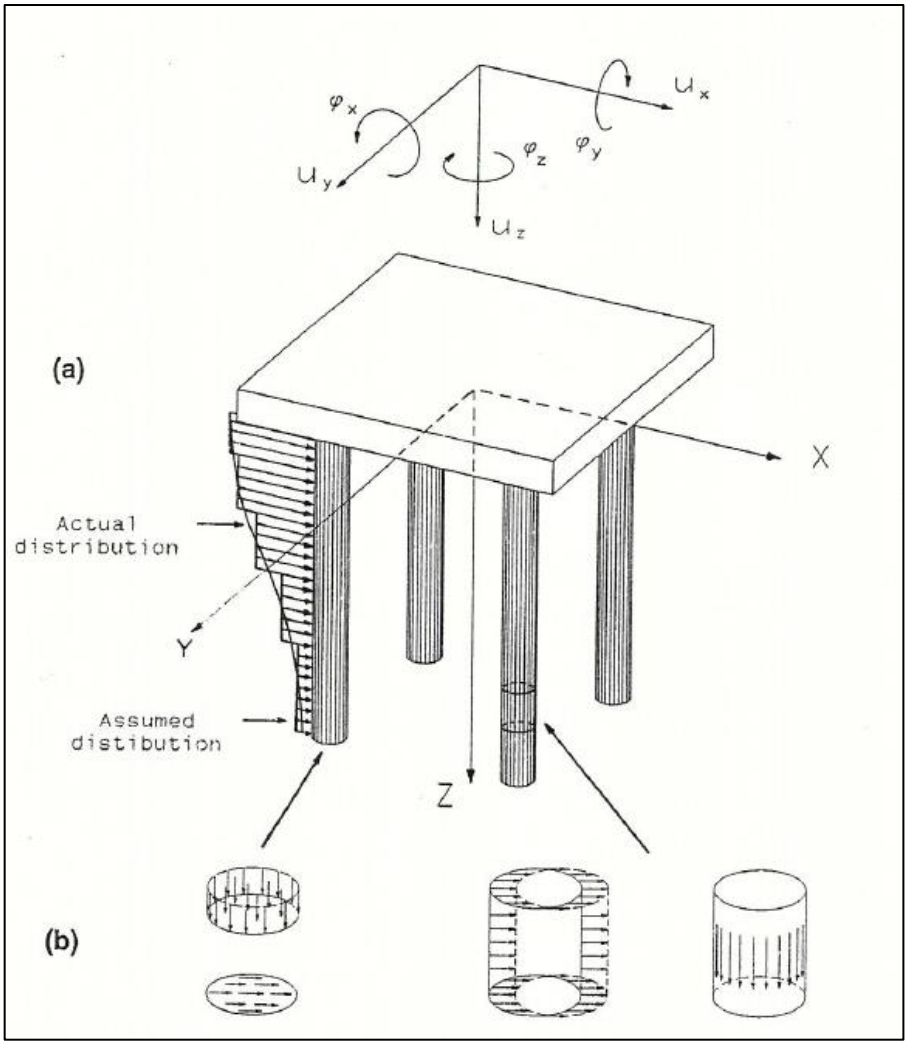

Figure 5: (a) Pile foundation interaction with the soil, (b) Barrel and disk loads representing pile/soil tractions. From (Kaynia & Kausel, 1991)

For each different piece of the pile, the force that applies on the node can be defined as (P) and the corresponding displacement as (U) and these can be expressed as:

$$P = \left(p_{1x}\ p_{1y}\ p_{1z} \dots\ p_{(\ell+1)x}\ p_{(\ell+1)y}\ p_{(\ell+1)z}\right) \tag{3.1}$$

$$U = \left(u_{1x}\ u_{1y}\ u_{1z} \dots\ u_{(\ell+1)x}\ u_{(\ell+1)y}\ u_{(\ell+1)z}\right) \tag{3.2}$$

According to these expressions the displacement, with a correlation of (P), and condition of both ends of the pile fixed can also be described as:

$$U = \Psi\, U_e + F_p\, P \tag{3.3}$$

Where

- $\Psi = (3(\ell + 1) \times 10)\ a\ shape\ matrix\ defining\ displacements\ of\ nodes\ in\ a\ fixed - end\ pile\ due\ to\ end\ displacements$
- $U_e = vector\ of\ displacements\ for\ the\ two\ ends\ of\ the\ pile$
- $F_p = flexibility\ matrix\ of\ pile\ under\ fixed - end\ condition$

The vector of displacements can be described as:

$$U_e = \left(u_{0x}\ \varphi_{0x} u_{0y} \varphi_{0y} u_{0z}\ u_{(\ell+1)x}\ \varphi_{(\ell+1)x} u_{(\ell+1)y} \varphi_{(\ell+1)y} u_{(\ell+1)z}\right) \tag{3.4}$$

By expressing the vector of external forces and moment (P_e) at the two of the pile by the dynamic stiffness matrix of the pile $\left(K_p\right)$ as:

$$P_e = K_p\, U_e - \Psi\, P \tag{3.5}$$

If considering the equilibrium between the soil and the forces $(-P)$ acting evenly on each piece of the pile as it was mentioned before, with the flexibility matrix of the soil (F_s), then:

$$U = -F_s\, P \tag{3.6}$$

By combining (3.3), (3.5) and (3.6) the following equations come up:

$$P_e = \left(K_p + \Psi \left(F_s + F_p\right)^{-1} \Psi\right) U_E \tag{3.7}$$

Or simply

$$P_e = K_e\, U_e \tag{3.8}$$

K_e is a matrix which relates the forces with the displacements at the ends of the pile.

4 CASE STUDY

4.1 GROUND CONDITIONS

Firstly, to define a model in any method the behaviour of the material, soil, must be described. There are several material models which are made for specific conditions, but most of them are describing the soil as a material with two mechanisms, elastic and plastic. These mechanisms are simply describing the strains that occur on the soil when it is loaded. So elastic strains are reversible, meaning that the soil will return to the initial state. On the other hand, the plastic strains are not reversible, and the deformation is permanent. In reality, the soil has a combination of these two mechanisms (Steinar, 2017). In this thesis the initial stiffness is considered therefore linear elastic material can describe the stiffness.

The basis for this model is given by Hook's law where the stiffness-strength relationship is:

$$E = \frac{\sigma}{\varepsilon} \tag{4.1}$$

For the linear elastic model, the parameters which are going to be used for this thesis will be presented below. It has to be noted that the soil will be a simulation of offshore water 30-35 meters deep condition. Which means that the values may vary from the typical values of the onshore soil.

Table 1: Basic soil parameters for offshore and undrained condition

Parameter	Unit	Value
Unit Weight [γ]	[kN/m^3]	14,50
Poisson's Ratio [ν]	[-]	0,495

Some other parameters which going to be used for this thesis but will be varying on respect to the elasticity modulus (E) will be listed below:

Table 2: Dynamic soil conditions; used for PILES program

Parameter	Unit
Shear Wave Velocity [v_s]	[m/s]
Shear Modulus [G]	[Pa]

These parameters can be calculated by the following formulas:

$$v_s = \sqrt{\frac{G}{\rho}} \tag{4.2}$$

$$G = \frac{E}{2\,(1+v)} \tag{4.3}$$

The elasticity of the soil can be expressed by shear stiffness modulus G or with the Young's modulus. That modulus varies with depth based on the mathematical equation:

$$E_s(z) = E_{ref}\left(\frac{z}{D}\right)^n \tag{4.4}$$

Where the reference stiffness E_{ref} is defined as the soil's Young modulus at the depth of one pile diameter. The exponential (n) defines the way the stiffness changes by depth. When $n = 0$ simulates a homogenous soil, close to over consolidation conditions. Then normal consolidated clay will behave with linear increase of the Young's modulus; thus, the exponential can be used as $n = 1$. Finally, a sand will usually behave with a parabolic increase of stiffness, so an $n = 0{,}5$ is the most appropriate value.

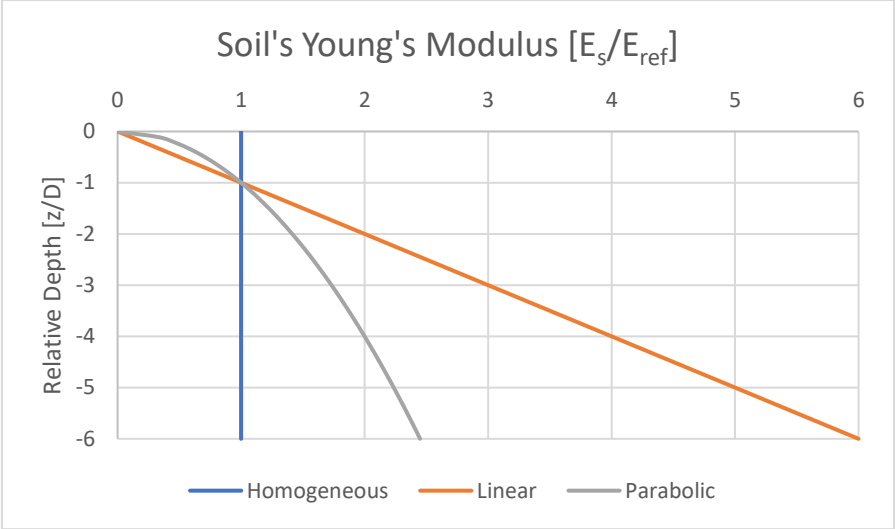

Figure 6: Soil profiles; homogeneous, linear & parabolic inhomogeneous

4.2 PILES PROGRAM MODEL

For this case study, a pile with constant diameter and wall thickness was modelled, the embedded length is changing from 18 to 54 meters with the interval of 9 meters. This gives ratios of length on diameter of the pile, from 2 to 6.

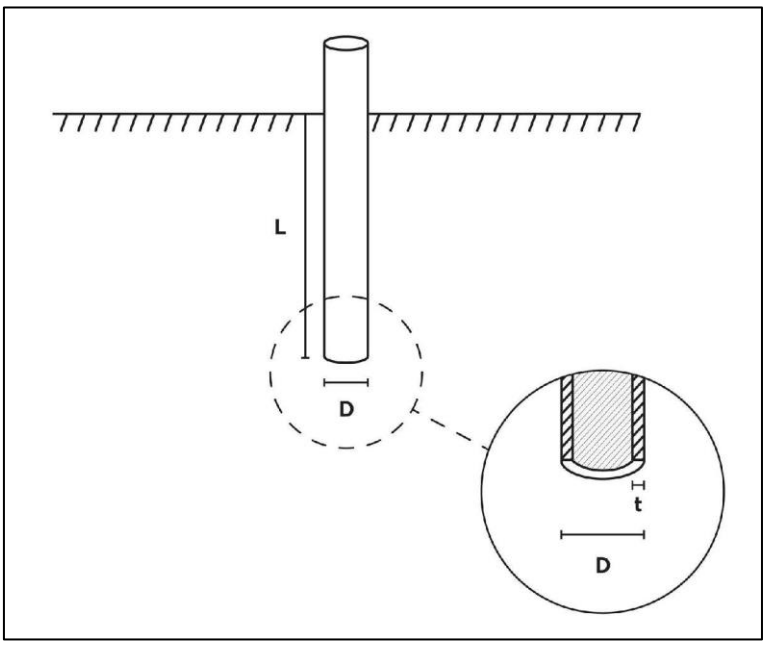

Figure 7:: The pile's dimensions

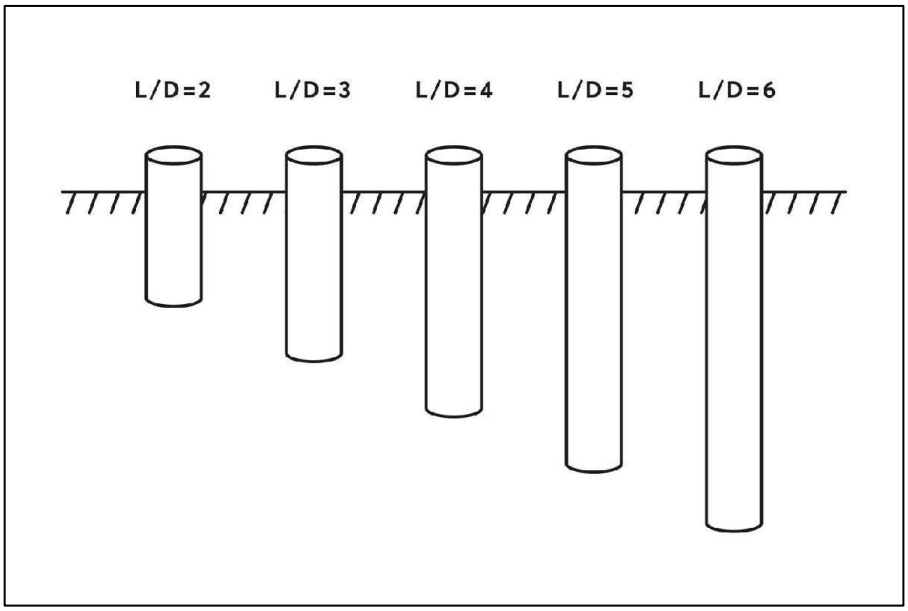

Figure 8:Pile ratios

Table 3: Pile dimensions

Pile Length	Ratio	Diameter	Thickness	Ratio
L	L/D	D	t	D/t
[m]	[-]	[m]	[m]	[-]
18	2	9	0,1125	80
27	3			
36	4			
45	5			
54	6			

As it can be seen from the table, the diameter and the thickness of the pile wall were kept constant, which also gives a constant ratio of the diameter over the thickness.

The steel parameters were chosen according to the international standards and the values are presented in the table below.

Table 4: Pile's steel parameters

Parameter	Unit	Value
Young's Modulus [E]	[Pa]	2,00E+11
Young's Modulus* [E*]	[Pa]	1,93E+10
Density [ρ]	[kg/m^3]	8,00E+03
Poisson's Ratio [ν]	[-]	0,3
EA	[N/m]	1,57E+11
EI	[N m^2/m]	6,20E+12

The characteristic Young's modulus $\left(E_p^*\right)$ of the pile. This parameter describes the elasticity of a solid pile as an equivalent of the stiffness of a hollow pile, it can be calculated by the formula:

$$E_p^* = E_p \left(1 - \left(\frac{r-t}{r}\right)^4\right) \tag{4.5}$$

Since only static analyses are carried out, the damping ratio is to be set as 0. The number of layers, in order to be applicable for all different pile lengths, were selected 19. Every layer has 3 meters thickness and beneath the layers, there is the half space. with the same soil parameters (Figure 9).

For this case study, three different soil profiles (Figure 6) were analysed

- Constant Soil Modulus
- Linear Increase Soil Modulus
- Parabolic Increase Soil Modulus

All these three will be determined below in details.

```
Piles - Notepad
File  Edit  Format  View  Help
Example Single Pile in a homogeneous half-space
   19    1
  03.0  30.1    1478.6    0.00   0.495
  03.0  30.1    1478.6    0.00   0.495
  03.0  30.1    1478.6    0.00   0.495
  03.0  30.1    1478.6    0.00   0.495
  03.0  30.1    1478.6    0.00   0.495
  03.0  30.1    1478.6    0.00   0.495
  03.0  30.1    1478.6    0.00   0.495
  03.0  30.1    1478.6    0.00   0.495
  03.0  30.1    1478.6    0.00   0.495
  03.0  30.1    1478.6    0.00   0.495
  03.0  30.1    1478.6    0.00   0.495
  03.0  30.1    1478.6    0.00   0.495
  03.0  30.1    1478.6    0.00   0.495
  03.0  30.1    1478.6    0.00   0.495
  03.0  30.1    1478.6    0.00   0.495
  03.0  30.1    1478.6    0.00   0.495
  03.0  30.1    1478.6    0.00   0.495
  03.0  30.1    1478.6    0.00   0.495
  03.0  30.1    1478.6    0.00   0.495
  0.00  30.1    1478.6    0.00   0.495
    1   0.0
   4.50    9
  1   1    9     1
    0.0     0.0      0.0
 1.57E11    6.20E12    305    0.3
   1    0    0    0
   1    0
```

Figure 9: Example of the PILES input data

4.2.1 Constant Stiffness with Depth

For constant soil modulus three different soil stiffness were studied, one soft clay with elasticity modulus at $4MPa$, a medium stiffness at $40MPa$ and a stiff soil with modulus at $140MPa$.

The PILES program has different input parameters than PLAXIS, so a conversion is needed. Firstly, the unit weight (γ) must change to density (ρ) using the formula $\gamma = \rho\, a_g$. Then the elasticity modulus must change first to shear modulus with equation (4.3) and then to shear wave velocity with equation (4.2).

4.2.2 Linear Increase Stiffness with Depth

For the linear inhomogeneous soil profile, there is no need for three different soil stiffness moduli to be studied. That is happening because the elasticity modulus is increasing linearly by depth. One of the soil that have this behaviour is the normally consolidated soils. Therefore, a reference soil modulus at the depth of one diameter of the pile will be

used to calculate the elasticity modulus at each depth using the formula (4.4) using the value (1,0) for n.

As before, the use of the input parameters for the PILES program will need the same conversions.

4.2.3 Parabolic Increase Soil Modulus

The parabolic inhomogeneous modulus will only use the reference elasticity modulus for the calculations with formula (4.4). In this case, the n will have the value (0,5). For a parabolic modulus increase, the simulation will be more relevant for a sand governing type of soil.

Finally, the same conversions at the input parameters will be used.

4.3 PLAXIS 3D

The program PILES was validated against the commercially available program PLAXIS 3D v. 2017. which is a three-dimension FE program specified for geotechnical problems.

4.3.1 Soil

The size of the soil volume was chosen based on the diameter and the length of the pile. So, the side boundaries of the soil box can be expressed as:

Table 5: Soil box dimensions For PLAXIS 3D

XX	YY	ZZ
22 D	11 D	6 L

These lengths are chosen big enough so there will be no influence from the boundaries of the soil model to the deflection of the pile.

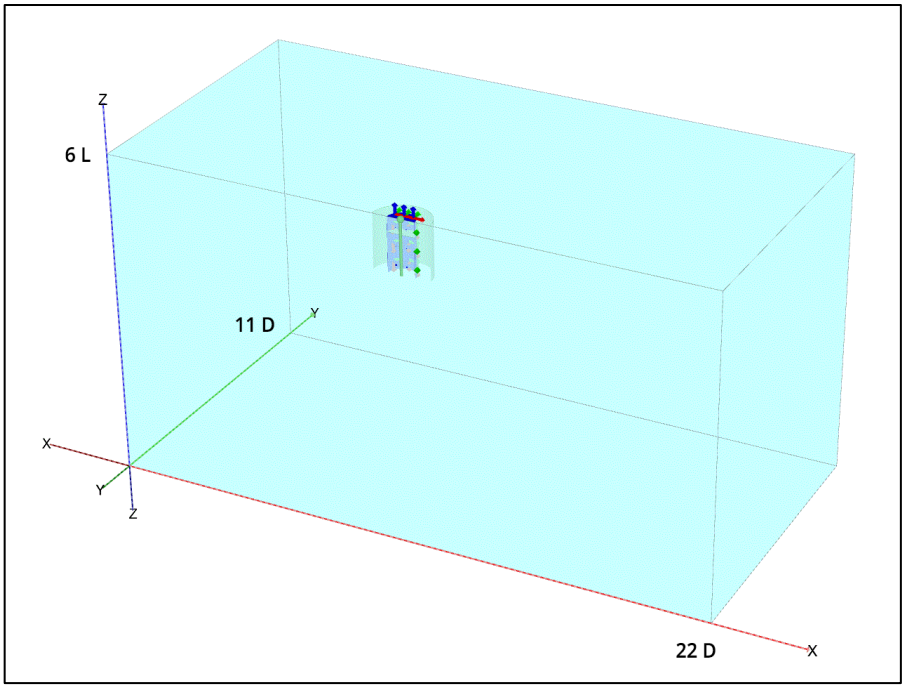

Figure 10: Model of the 18m pile at PLAXIS 3D

Also, the model was made symmetric around the xz plane, that way the demand on computer power and computing time will be significant lower. Consequently, the results will be valid for the half model. Thus, an adjustment to the actual results is needed.

The soil was modelled according to the *table 1* on undrained conditions, justifying the Poisson's ratio $\nu = 0{,}495$. The water level was set to be the same with the soil surface as it represents deep sea conditions.

4.3.2 Pile

The monopile was modelled as a half circular plate. At the mudline a lid was placed on the top of the pile, which was chosen as a rigid body. The reason for that is to have a better distribution of the stresses along the pile. The rest of the pile has the material properties of steel based on *table 4*.

4.3.3 Elements

The following types of elements was used in the analyses.

Table 6: Default elements in PLAXIS 3D

Type	Nodes	Shape
Soil	10	Tetrahedral
Plate	6	Triangular

4.3.4 Mesh

The mesh distribution was selected medium, but for better resolution around the pile, where is the most important area, the coarseness factor for all plates selected 0,1. Then for the soil, the coarseness factor is 0,7. The soil volume closer to the pile is gradually finer. The element size for all the models varies between 35 and 40 thousand elements.

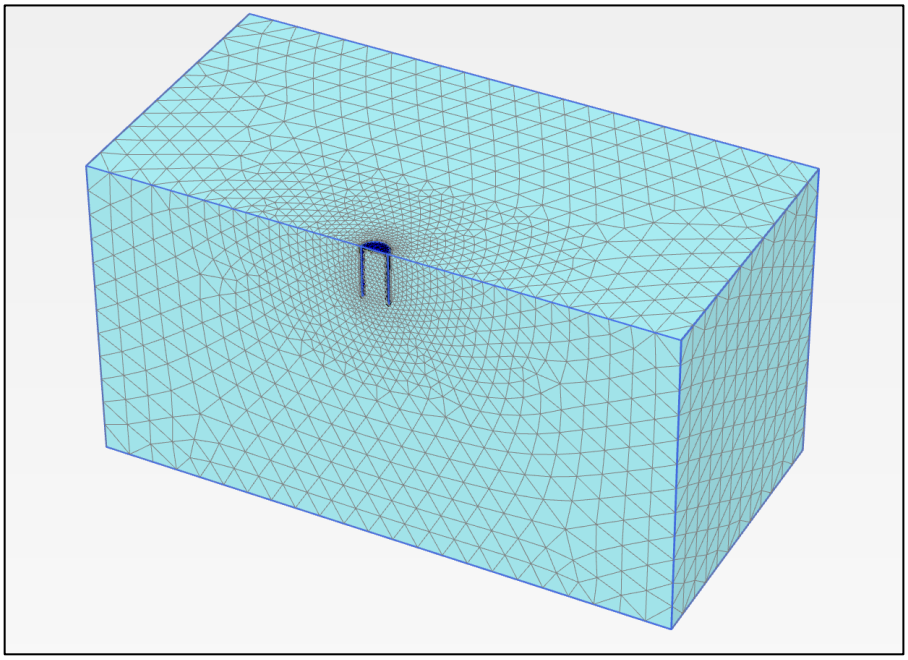

Figure 11: Mesh for the 18 meters pile model

4.3.5 Load Characteristics

The simulation is for this study considers only lateral loading, thus the loads that are important for the model are the horizontal and the bending moment around the loading axis.

The following load was used in the validation. The load where applied at seabed level:

- $F_h = 500\ kN$ On the X axis
- $M = 70\ MN$ Around Y axis and with positive trend

4.3.6 Stage Construction

The simulation in PLAXIS has divided 5 stages.

- The *Initial Phase* initiate the stresses in the soil by the *K0 procedure*
- Phase 2 the *Pile Installation* phase where the pile together with the interfaces are activated by "wished in place".
- Phase 3 applying Horizontal Load, F
- Phase 4 Applying overturing moment, M
- Phase 5 Applying the Combination of Loads, F and M

All the three load phases start from the *Installation Phase (Phase 1)*.

5 VALIDATION

The validation method for the PILES program was carried out in four stages. Firstly, an analysis with the program PILES based on the case study which was presented in the previous chapter. The second stage is to use the same soil and pile parameters for an analysis with closed form solutions which were presented in chapter 2.4. These formulas will be used to obtain results for rigid and flexible piles. But one of the main problems of using just these formulas is that these formulas are describing either pure rigid or pure flexible conditions but do not calculate the grey zone between these two conditions, and offshore monopiles are in this "grey zone" in many cases. Consequently, this leads to stage three, where results from the finite element program PLAXIS 3D will be used. This program will be vital to calculate the response in this "grey zone". Finally, the last stage is to compare all the previous method and prove that PILES program can efficient be used for calculating the stiffens.

5.1 PILES PROGRAM

The PILES program output is giving directly the stiffness matrix of the system soil/pile. The results are based on a six degree of freedom system with forces, bending moment, translation and rotation acting in a three-direction (x, y, z) model as it was presented in chapter 3.

The table results are given in six double columns and six rows. For the double columns each second part shows the dynamic analysis of the pile, but at this study, it is zero in every cell due to the damping ratio being also zero, so only the first part is useful. The labels starting from the upper left cell are giving alternate the translation and rotation stiffness coefficient for each direction $(U_x, U_{xz}, U_y, U_{yz}, U_z, U_{zz})$.

Where

- $U_x = translation\ in\ x\ direction$
- $U_{xz} = ratation\ in\ the\ xz\ plane$
- $U_y = translation\ in\ y\ direction$
- $U_{yz} = ratation\ in\ the\ yz\ plane$
- $U_z = translation\ in\ z\ direction$
- $U_{zz} = ratation\ in\ the\ xy\ plane$

From these values, the important ones for the study are located at the cells (U_x, U_x) for the horizontal stiffness coefficient K_F. Then the cell (U_{xz}, U_{xz}) gives the value for the bending moment stiffness K_M. Finally, for the coupling term the cells (U_{xz}, U_x) and (U_x, U_{xz}) give the value for K_C. It has to be noted that due to the unusual axis orientation, the K_C gives a positive value and not a negative as it is expected to give. Finally, all the values are given in a scientific form.

5.1.1 Constant Soil Modulus

For the soil profile with a constant elasticity modulus, three different soil stiffnesses soft ($4\ MPa$), medium ($40\ MPa$) and stiff ($140\ MPa$) were analyzed.

After assembling all the results from every pile length for the soft clay ($4\ MPa$) the following stiffness coefficients are presented.

Table 7: PILES results for stiffness coefficients for homogeneous soft soil (4MPa)

Stiffness Coefficients			
Length	Horizontal	Rotation	Coupling
L [m]	K_F [Pa m]	K_M [Pa m^3]	K_C [Pa m^2]
18	1,30E+08	2,56E+10	-1,40E+09
27	1,62E+08	6,36E+10	-2,50E+09
36	1,85E+08	1,14E+11	-3,57E+09
45	1,97E+08	1,66E+11	-4,36E+09
54	2,02E+08	2,06E+11	-4,78E+09

The same procedure is taking place for the medium ($40\ MPa$) and stiff ($140\ MPa$) soil.

Table 8: PILES results for stiffness coefficients for homogeneous medium soil (40MPa)

Stiffness Coefficients			
Length	Horizontal	Rotation	Coupling
L [m]	K_F [Pa m]	K_M [Pa m^3]	K_C [Pa m^2]
18	1,20E+09	2,14E+11	-1,19E+10
27	1,30E+09	3,76E+11	-1,59E+10
36	1,31E+09	4,50E+11	-1,65E+10
45	1,31E+09	4,68E+11	-1,62E+10
54	1,33E+09	4,70E+11	-1,60E+10

Table 9: PILES results for stiffness coefficients for homogeneous stiff soil (140MPa)

Stiffness Coefficients			
Length	Horizontal	Rotation	Coupling
L [m]	K_F [Pa m]	K_M [Pa m^3]	K_C [Pa m^2]
18	3,65E+09	5,19E+11	-3,06E+10
27	3,68E+09	6,49E+11	-3,20E+10
36	3,72E+09	6,64E+11	-3,13E+10
45	3,79E+09	6,64E+11	-3,14E+10
54	3,82E+09	6,66E+11	-3,16E+10

5.1.2 Linear Increase Soil Modulus

For the soil profile with a linear inhomogeneous elasticity modulus, the use of the reference Young's modulus E_{ref} at depth of one pile diameter is needed. For this study, the reference stiffness set at $4\ MPa$ and the following results are presented:

Table 10: PILES results for stiffness coefficients for linear inhomogeneous soil with reference value at 4MPa

Stiffness Coefficients			
Length	Horizontal	Rotation	Coupling
L [m]	K_F [Pa m]	K_M [Pa m^3]	K_C [Pa m^2]
18	2,35E+08	5,30E+10	-3,13E+09
27	3,53E+08	1,62E+11	-6,69E+09
36	4,07E+08	2,80E+11	-9,18E+09
45	4,13E+08	3,43E+11	-9,75E+09
54	4,16E+08	3,61E+11	-9,58E+09

5.1.3 Parabolic Increase Soil Modulus

Finally, at the parabolic increase soil stiffness profile the reference Young's modulus E_{ref} will be used again with the same value of 4 MPa. The results are presented below:

Table 11: PILES results for stiffness coefficients for parabolic inhomogeneous soil with reference value at 4MPa

Stiffness Coefficients			
Length	Horizontal	Rotation	Coupling
L [m]	K_F [Pa m]	K_M [Pa m^3]	K_C [Pa m^2]
18	1,72E+08	3,64E+10	-2,10E+09
27	2,37E+08	1,02E+11	-4,15E+09
36	2,76E+08	1,85E+11	-5,96E+09
45	2,90E+08	2,52E+11	-6,89E+09
54	2,91E+08	2,88E+11	-7,08E+09

5.2 STIFFNESS FORMULAS

The procedure of validation of the PILES program includes the comparison of the results with the formulas from the subchapter 2.5. As it was mentioned before, these formulas fail to capture the behaviour of piles which do not have definite flexible or rigid response to loading. So,

by using these formulas for validation it will be possible to confirm the trend behaviour of the piles from a rigid situation to a flexible one.

For all three different soil profiles, the calculations for the flexible pile condition was based on the Gazetas formulas (Gazetas, 1984). Since the flexible piles are independent of the total length, the values for all pile lengths are the same.

So, the results for a flexible pile in soft soil ($4\ MPa$) are presented below:

Table 12: Stiffness coefficients for slender pile in soft homogeneous soil

Stiffness Coefficients		
Slender (Gazetas, 1984)		
Horizontal	Rotation	Coupling
K_F [Pa m]	K_M [Pa m^3]	K_C [Pa m^2]
2,31E+08	2,70E+11	-4,95E+09

As for the rigid condition of the pile the formulation from Shadlou will be used (Shadlou & Bhattacharya, 2016). These formulas are depending on the pile length, so the analysis will be for the lengths form $18 - 54$ with the interval of 9 meters.

So, the results for a rigid pile in soft soil ($4\ MPa$) are presented below:

Table 13: Stiffness coefficients for rigid pile in soft homogeneous soil

Stiffness Coefficients			
Rigid (Shadlou & Bhattacharya, 2016)			
Length	Horizontal	Rotation	Coupling
L [m]	K_F [Pa m]	K_M [Pa m^3]	K_C [Pa m^2]
18	1,42E+08	2,19E+10	-1,30E+09
27	1,83E+08	6,02E+10	-2,46E+09
36	2,19E+08	1,24E+11	-3,85E+09
45	2,51E+08	2,16E+11	-5,45E+09
54	2,81E+08	3,41E+11	-7,24E+09

This study considered all three soil profiles. But in this chapter only the results from the homogeneous soft soil are presented. The rest of the results are available in the appendix at tables $26 - 33$.

5.3 PLAXIS 3D

Based on the parameters which were proposed in the subchapter 4.3, a basic soil model was established with the capability to change the length of the pile but keeping the diameter constant. For that analysis, the soil was chosen as soft clay with constant elasticity modulus at $4\ MPa$.

Though, PLAXIS 3D cannot give the results in the form of stiffness matrix, as the program PILES do. So, a specific procedure was adopted in order to calculate the stiffness.

The analysis in PLAXIS was made in three different load combinations, only horizontal load, only bending moment and the combination of these two together. That way gives the flexibility to extract values from a specific load combination.

So, from all three load combinations, the results for the horizontal displacement on the mudline level was extracted from PLAXIS. The results are presented below:

Table 14: Values of horizontal displacement for all load combinations

l [m]	u_F [m]	u_M [m]	u_T [m]
18	0,01773	0,13830	0,15600
27	0,01542	0,89310	0,10470
36	0,01365	0,06340	0,07705
45	0,01228	0,04836	0,06065
54	0,01122	0,03898	0,05020

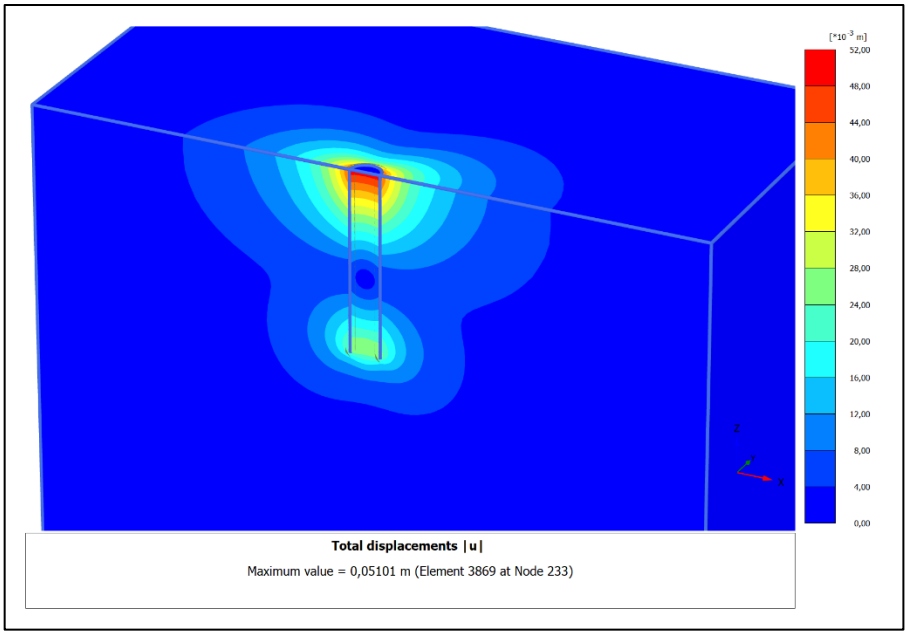

Figure 12: Graphic display of total displacement for an 18-meter-long pile is soft homogeneous soil

To calculate the inclination of the pile head at the mudline level a similar procedure with the displacement took place. But there is no output to give the inclination in PLAXIS. So, results extracted by measuring the position change of the two rear nodes at the top of the pile, see picture 13. Also, the values which the program gives are in degrees, so for further calculations, these values must be transformed to radians. The initial values and the altered ones are presented in the table below:

Table 15: Values of inclination in rad & degrees for all load combinations

l	θ_F	θ_M	θ_T	θ_F	θ_M	θ_T
[m]	[deg]	[deg]	[deg]	[rad]	[rad]	[rad]
18	0,057	0,762	0,819	9,95E-04	1,33E-02	1,43E-02
27	0,037	0,341	0,378	6,46E-04	5,95E-03	6,60E-03
36	0,026	0,192	0,218	4,54E-04	3,35E-03	3,80E-03
45	0,020	0,126	0,146	3,49E-04	2,20E-03	2,55E-03
54	0,016	0,094	0,110	2,79E-04	1,64E-03	1,92E-03

Now it is needed to calculate the stiffness coefficients of the system soil/pile from the results above. The is presented analytically below:

From the following equations to calculate the deformation on the pile

$$u_T = \frac{K_M}{K_F\, K_M - K_C^2} F - \frac{K_C}{K_F\, K_M - K_C^2} M \tag{5.1}$$

$$\theta_T = \frac{K_F}{K_F\, K_M - K_C^2} M - \frac{K_C}{K_F\, K_M - K_C^2} F \tag{5.2}$$

the partial deformations can be calculated when one of the loads, the horizontal force or the bending moment, is not applied on the pile. So firstly, if only the lateral force is applied the equation (5.1) will have the form:

$$u_F = \frac{K_M}{K_F\, K_M - K_C^2} F \tag{5.3}$$

and then by separating the coefficients with the force and the displacement, the result is:

$$\frac{K_M}{K_F\, K_M - K_C^2} = \frac{u_F}{F} \tag{5.4}$$

Again, the same procedure is taking place by applying only the bending moment on the pile. This leads to the equation (5.2) having the form:

$$\theta_M = \frac{K_F}{K_F\, K_M - K_C^2} M \tag{5.5}$$

and as before, by separating the coefficients from the force and the deformation, the result is:

$$\frac{K_F}{K_F\,K_M - K_C^2} = \frac{\theta_M}{M} \tag{5.6}$$

Finally, for the coefficient K_C a different approach must take place. That is to divide the equation (5.1) with the (5.2) which leads to:

$$\frac{u_T}{\theta_T} = \frac{\frac{K_M}{K_F\,K_M - K_C^2}F - \frac{K_C}{K_F\,K_M - K_C^2}M}{\frac{K_F}{K_F\,K_M - K_C^2}M - \frac{K_C}{K_F\,K_M - K_C^2}F} \tag{5.7}$$

and by solving (5.7) on respect to K_C the equation that comes is:

$$\frac{K_C}{K_F\,K_M - K_C^2} = \frac{\theta_T\,\frac{K_M}{K_F\,K_M - K_C^2}\,F - u_T\,\frac{K_F}{K_F\,K_M - K_C^2}\,M}{\theta_T\,M - u_T\,F} \tag{5.8}$$

By using the results from the tables 22 and 23, along with the equations (5.4), (5.6) and (5.8), the following table is formed.

Table 16: 3X3 equation system with the values sorted by pile length

L [m]	$\frac{K_F}{K_F\,K_M - K_C^2}$	$\frac{K_M}{K_F\,K_M - K_C^2}$	$\frac{K_C}{K_F\,K_M - K_C^2}$
18	1,90E-10	3,55E-08	-1,97E-09
27	8,50E-11	3,08E-08	-1,27E-09
36	4,79E-11	2,73E-08	-9,05E-10
45	3,14E-11	2,46E-08	-6,90E-10
54	2,34E-11	2,24E-08	-5,56E-10

This table has values from three equations, where all the equations have the same three unknowns. By solving the system of $3x3$ and then multiply the results by 2* the following table of results for the stiffness coefficients comes up:

Table 17: Stiffness coefficient values from PLAXIS 3D

L [m]	K_F [Pa m]	K_M [Pa m^3]	K_C [Pa m^2]
18	1,33E+08	2,48E+10	-1,38E+09
27	1,69E+08	6,13E+10	-2,53E+09
36	1,96E+08	1,12E+11	-3,70E+09
45	2,12E+08	1,66E+11	-4,66E+09
54	2,18E+08	2,08E+11	-5,17E+09

*The multiplication is happening because the PLAXIS 3D model is axisymmetric along the plane xz, so all the results must be multiplied by 2 to be corrected and obtain the actual ones.

5.4 COMPARISON OF THE RESULTS AND VALIDATION

Now the validation of the program PILES can be accomplished by comparing the results from all the methods for the same case study and conditions of the soil and the pile.

For the comparison of the results the homogeneous soft soil $(4MPa)$profile was chosen. The properties of the embedded pile and steel properties were chosen as they were discussed at the case study. Thus, a diameter of 9 meters and the length varies from 18 to 54 meters with the interval of 9 meters.

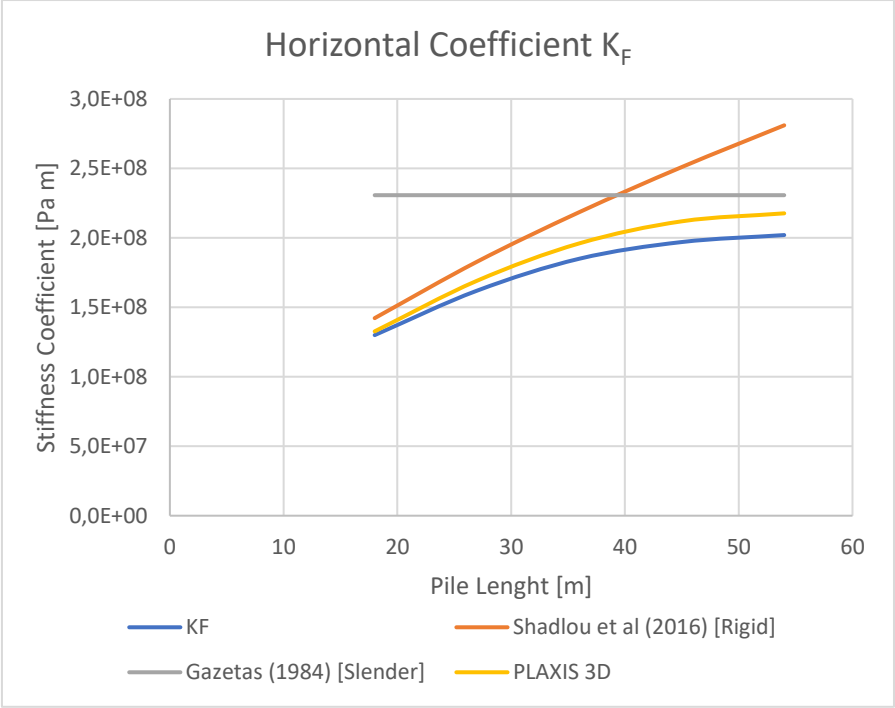

Figure 13: Results of horizontal stiffness change by pile length for homogeneous soil

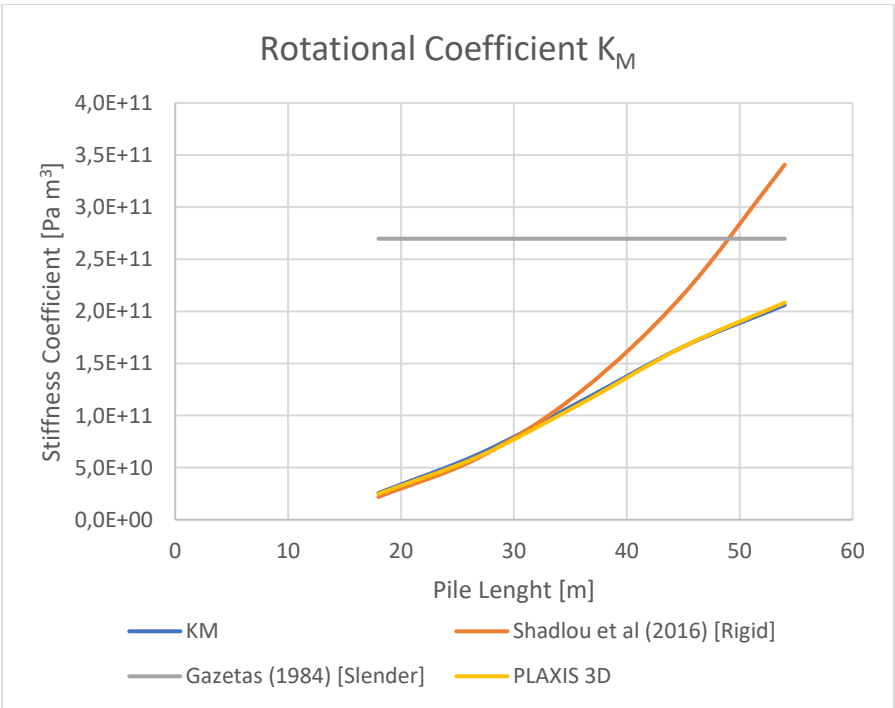

Figure 14: Results of rotational stiffness change by pile length for homogeneous soil

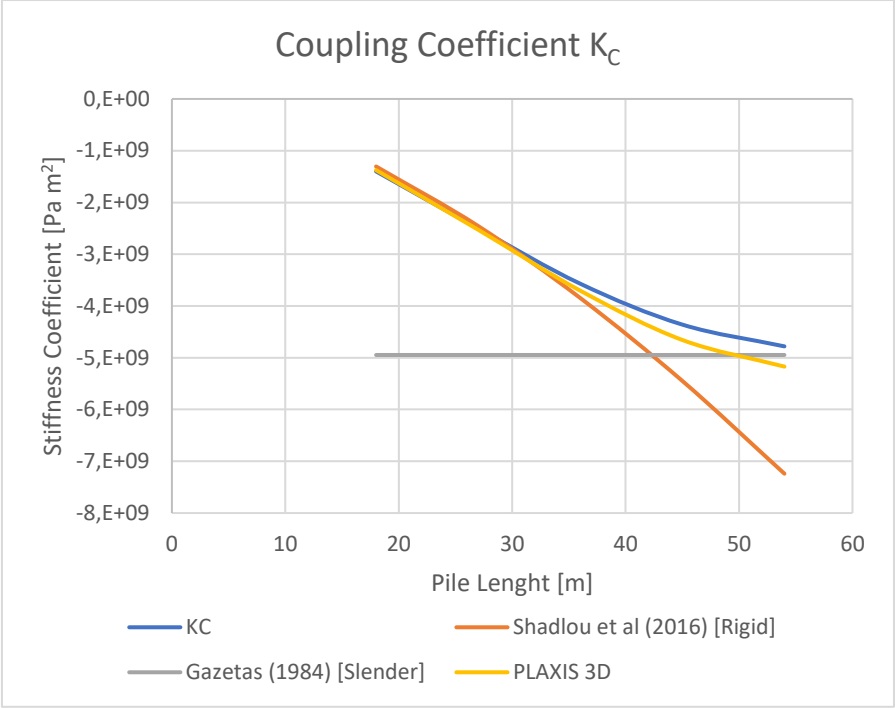

Figure 15: Results of coupling stiffness change by pile length for homogeneous soil

From the graphs, it can be noticed that the rotation coefficient K_M has almost the same values for all the lengths of the pile for the program PILES and PLAXIS 3D. The horizontal coefficient K_F starts with almost no difference with PLAXIS 3D but gradually the difference is increased to reach less than 10% variation. This is happening while the length of the pile is increasing. Similar behaviour can be observed for the coupling coefficient K_C, where it has the same results at the shorter pile lengths and the difference is increasing when the pile length is also increasing. Although the variation does not reach the same level as at the horizontal coefficient.

Also, it can be seen that the behaviour of the sorter piles is following the expressions for rigid piles, but when the length is increasing it tends to follow the formulas for the slender piles, which is independent of the total length of the pile.

The results from the other two nonhomogeneous soil profiles are not presented here. The reason is that the analysis at the PLAXIS program has made for the homogeneous soil profile. Although the graphs with results are in the appendix and one can see that the same pattern is happening for all the other results. That means that the PILES program results have a more rigid behaviour for short pile and more flexible for longer piles. Also, when the soil is becoming stiffer the behaviour turns to be more flexible. Concluding the potential use of the program PILES and the upcoming method will be more suitable for piles with intermediate behaviour and soil profiles with normal consolidated clays or overconsolidated clays with a low degree of consolidation.

6 DESIGN METHODOLOGY

In this section of the thesis, it is proposed a methodology to calculate fast the monopile stiffness of the pile head at the mudline, while it is loaded laterally. As it was previous mentioned, there is an undefined range in the literature between of the rigid pile and the flexible pile behaviour. This range is relevant for OWT monopile dimensions.

Now that it is proved that the program PILES can accurately calculate the stiffness coefficients, a different analysis approach is needed to construct a methodology to calculate the stiffness. For that reason, it is necessary to take results for extremely low elasticity values to extremely high ($20\ kPa\ to\ 100\ GPa$) to cover all the range of stiffness values. Therefore, with the program PILES an analysis was conducted with the same soil profiles. One homogeneous, one linear inhomogeneous and one parabolic inhomogeneous increase of stiffness. The pile had the same steel properties. Also piles with different diameters were studied, but with the same ratio of length on diameter.

6.1 RESULTS

Before presenting the results, which will be the base for the methodology, it must be mentioned that the ratio of the length on the diameter (L/D) of the pile will be used as a guideline for this methodology. So, the lengths which were used in the case study for the validation and for the basis of this method, will have the following form:

Table 18: Pile dimensions ratios correspond to case study pile lengths

Length [L]	Ratio [L/D]
18	2
27	3
36	4
45	5
54	6

The results from the PILES program were obtained for every different pile length. The analyses took place with soil elasticity modulus varies from the extremely low value to the extremely high value ($20\ kPa\ to\ 100\ GPa$) for homogeneous soil profile.

The results are listed by the elasticity modulus values and by the ratio (L/D). Thus, all these values in the tables 27-29 are not normalized yet and they are characteristic values for the pile with diameter of 9 meters.

Table 19: Results for horizontal stiffness for the chosen case study

Horizontal Stiffness Coefficient K_F					
Elasticity [Pa]	Ratio L/D				
	2	3	4	5	6
2,0E+04	6,4E+05	8,2E+05	1,0E+06	1,2E+06	1,3E+06
2,0E+05	6,5E+06	8,4E+06	1,0E+07	1,2E+07	1,3E+07
4,0E+06	1,3E+08	1,6E+08	1,9E+08	2,0E+08	2,0E+08
4,0E+07	1,2E+09	1,3E+09	1,3E+09	1,3E+09	1,3E+09
1,4E+08	3,7E+09	3,7E+09	3,7E+09	3,8E+09	3,8E+09
1,0E+09	1,9E+10	2,0E+10	2,0E+10	2,0E+10	2,0E+10
1,0E+10	1,5E+11	1,5E+11	1,5E+11	1,5E+11	1,5E+11
1,0E+11	1,1E+12	1,1E+12	1,1E+12	1,1E+12	1,1E+12

Table 20: Results for rotational stiffness for the chosen case study

Rotation Stiffness Coefficient K_M					
Elasticity [Pa]	Ratio L/D				
	2	3	4	5	6
2,0E+04	1,3E+08	3,4E+08	6,8E+08	1,2E+09	1,9E+09
2,0E+05	1,3E+09	3,4E+09	6,9E+09	1,2E+10	1,9E+10
4,0E+06	2,6E+10	6,4E+10	1,1E+11	1,7E+11	2,1E+11
4,0E+07	2,1E+11	3,8E+11	4,5E+11	4,7E+11	4,7E+11
1,4E+08	5,2E+11	6,5E+11	6,6E+11	6,6E+11	6,7E+11
1,0E+09	1,2E+12	1,2E+12	1,2E+12	1,2E+12	1,2E+12
1,0E+10	2,2E+12	2,2E+12	2,2E+12	2,2E+12	2,2E+12
1,0E+11	4,1E+12	4,1E+12	4,1E+12	4,1E+12	4,1E+12

Table 21: Results for coupling stiffness for the chosen case study

Coupling Stiffness Coefficient K_C					
Elasticity [Pa]	Ratio L/D				
	2	3	4	5	6
2,0E+04	-7,0E+06	-1,3E+07	-2,1E+07	-3,0E+07	-4,1E+07
2,0E+05	-7,1E+07	-1,3E+08	-2,1E+08	-3,0E+08	-4,0E+08
4,0E+06	-1,4E+09	-2,5E+09	-3,6E+09	-4,4E+09	-4,8E+09
4,0E+07	-1,2E+10	-1,6E+10	-1,7E+10	-1,6E+10	-1,6E+10
1,4E+08	-3,1E+10	-3,2E+10	-3,1E+10	-3,1E+10	-3,2E+10
1,0E+09	-9,1E+10	-9,1E+10	-9,2E+10	-9,2E+10	-9,2E+10
1,0E+10	-3,4E+11	-3,4E+11	-3,4E+11	-3,4E+11	-3,4E+11
1,0E+11	-1,4E+12	-1,4E+12	-1,4E+12	-1,4E+12	-1,4E+12

The same procedure took place for the linear and parabolic inhomogeneous profiles. The tables of results for these profiles are listed in the appendix at figures $22 - 33$.

6.2 NORMALIZATION PROCESS

It is important when a method is proposed, to be applicable in general dimension conditions. For that reason, the stiffness coefficient results from one case study must be normalized. As it was mentioned before the ratio of the length on the diameter (L/D) of the pile will be used as a guideline for the methodology. Thus, the normalization will be achieved on respect to the diameter (D).

Therefore, the results from the subchapter 6.1 will go through the normalization procedure based on the reference elasticity modulus and the length/diameter ratios. Consequently, the new dimensionless coefficients will be k_F, k_M and k_C for horizontal, moment and coupling respectively.

The normalization for the stiffness coefficients was applied as shown below:

$$k_F = \frac{K_F}{E_{ref}\, D} \tag{6.1}$$

$$k_M = \frac{K_M}{E_{ref}\ D^3} \tag{6.2}$$

$$k_C = \frac{K_C}{E_{ref}\ D^2} \tag{6.3}$$

In respect to this normalization process, the following tables are showing the dimensionless coefficient factors k_i for a variation of soil stiffness and for the five different dimension ratios.

Table 22: Normalized horizontal stiffness values

Dimensionless Horizontal Stiffness Coefficient k_F					
Elasticity [Pa]	Ratio L/D				
	2	3	4	5	6
2,0E+04	3,56	4,58	5,54	6,44	7,33
2,0E+05	3,62	4,65	5,61	6,50	7,33
4,0E+06	3,61	4,50	5,14	5,47	5,61
4,0E+07	3,33	3,61	3,64	3,64	3,69
1,4E+08	2,90	2,92	2,95	3,01	3,03
1,0E+09	2,16	2,20	2,21	2,21	2,21
1,0E+10	1,61	1,61	1,61	1,61	1,61
1,0E+11	1,22	1,22	1,22	1,22	1,22

Table 23: Normalized rotational stiffness values

Dimensionless Rotation Stiffness Coefficient k_M					
Elasticity [Pa]	Ratio L/D				
	2	3	4	5	6
2,0E+04	8,71	23,05	46,78	82,30	130,32
2,0E+05	8,92	23,39	47,19	81,62	127,57
4,0E+06	8,78	21,81	39,09	56,93	70,64
4,0E+07	7,34	12,89	15,43	16,05	16,12
1,4E+08	5,09	6,36	6,51	6,51	6,53
1,0E+09	1,58	1,58	1,59	1,59	1,59
1,0E+10	0,30	0,30	0,30	0,30	0,30
1,0E+11	0,06	0,06	0,06	0,06	0,06

Table 24: Normalized coupling stiffness values

Dimensionless Coupling Stiffness Coefficient k_C					
Elasticity [Pa]	Ratio L/D				
	2	3	4	5	6
2,0E+04	-4,29	-8,09	-12,84	-18,58	-25,12
2,0E+05	-4,36	-8,21	-12,96	-18,52	-24,69
4,0E+06	-4,32	-7,72	-11,02	-13,46	-14,75
4,0E+07	-3,67	-4,91	-5,09	-5,00	-4,94
1,4E+08	-2,70	-2,82	-2,76	-2,77	-2,79
1,0E+09	-1,13	-1,13	-1,14	-1,14	-1,14
1,0E+10	-0,41	-0,41	-0,41	-0,41	-0,41
1,0E+11	-0,18	-0,18	-0,18	-0,18	-0,18

Furthermore, because the EA and EI of each pile is changing with different pile dimensions, an additional parameter must be used. This parameter is named "Correction Factor" and it is symbolised with γ and with index a F, M, or C for horizontal, moment and coupling respectively. This factor is showing the rate of change of the dimensionless coefficient k_i in respect of the length on diameter ratio of the pile. So, it is expressed as:

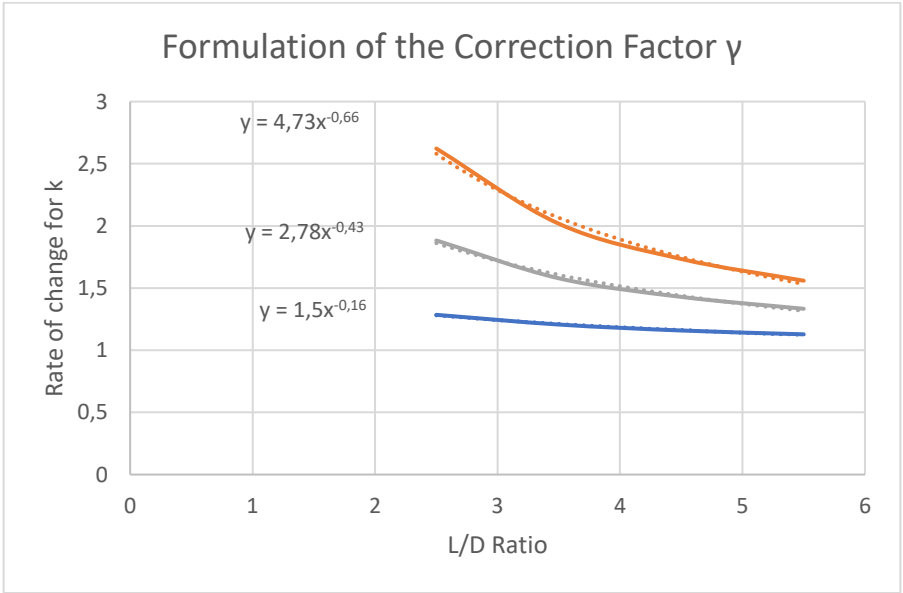

Figure 16: Identification of the Correction Factor γ

Here are listed the formulas to calculate the diameter factor:

$$\gamma_F = 1{,}5 \times \left(\frac{L}{D}\right)^{-0{,}16} \tag{6.4}$$

$$\gamma_M = 4{,}73 \times \left(\frac{L}{D}\right)^{-0{,}66} \tag{6.5}$$

$$\gamma_C = 2{,}78 \times \left(\frac{L}{D}\right)^{-0{,}43} \tag{6.6}$$

This factor is multiplied with the dimensionless coefficients k_i in order to correct the design values for the stiffness coefficients K_i.

Finally, the dimensionless coefficient J is proposed for this methodology. This dimensionless coefficient is a normalized stiffness ratio of the pile over the soil and it is defined as:

$$J = \frac{E_p^*}{E_s}\left(\frac{L}{D}\right) \tag{6.7}$$

The results based on the dimensionless coefficient J and on each different direction and the coupling stiffness is presented below:

Table 25: Values for the dimensional coefficient J

Dimensionless Coefficient J					
Elasticity [Pa]	Ratio L/D				
	2	3	4	5	6
2,0E+04	1,9E+06	2,9E+06	3,9E+06	4,8E+06	5,8E+06
2,0E+05	1,9E+05	2,9E+05	3,9E+05	4,8E+05	5,8E+05
4,0E+06	9,6E+03	1,4E+04	1,9E+04	2,4E+04	2,9E+04
4,0E+07	9,6E+02	1,4E+03	1,9E+03	2,4E+03	2,9E+03
1,4E+08	2,8E+02	4,1E+02	5,5E+02	6,9E+02	8,3E+02
1,0E+09	3,9E+01	5,8E+01	7,7E+01	9,6E+01	1,2E+02
1,0E+10	3,9E+00	5,8E+00	7,7E+00	9,6E+00	1,2E+01
1,0E+11	3,9E-01	5,8E-01	7,7E-01	9,6E-01	1,2E+00

6.3 THE CHARTS

With the results from the normalized dimensionless stiffness coefficient k_i and with the dimensionless coefficient J, groups of charts were designed to be used for calculation of the stiffness coefficients K_i of monopiles.

Here will be presented the charts for the homogeneous soil profile. Although, the charts for all three soil profiles are available in the appendix of this thesis at figures $34 - 42$.

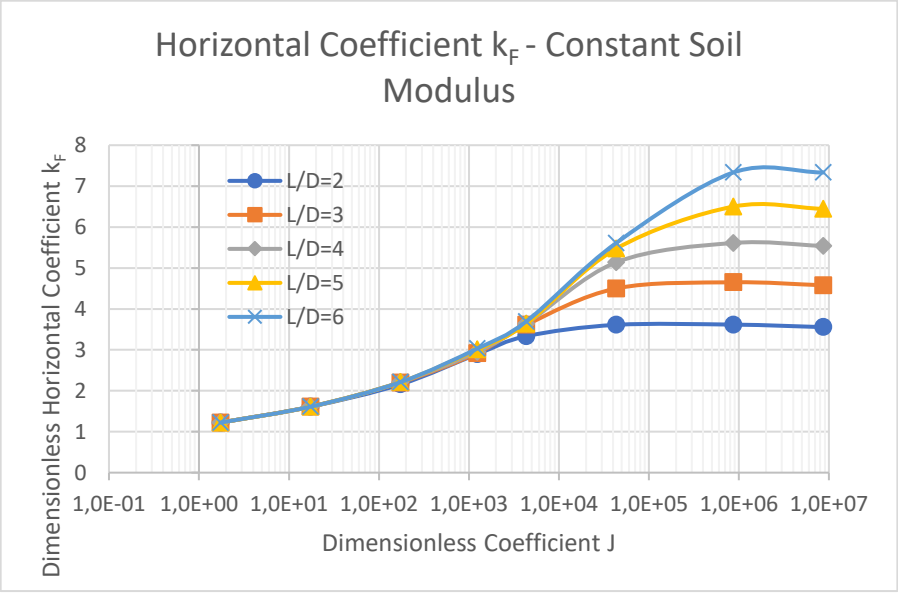

Figure 17: Normalized chart of the horizontal stiffness

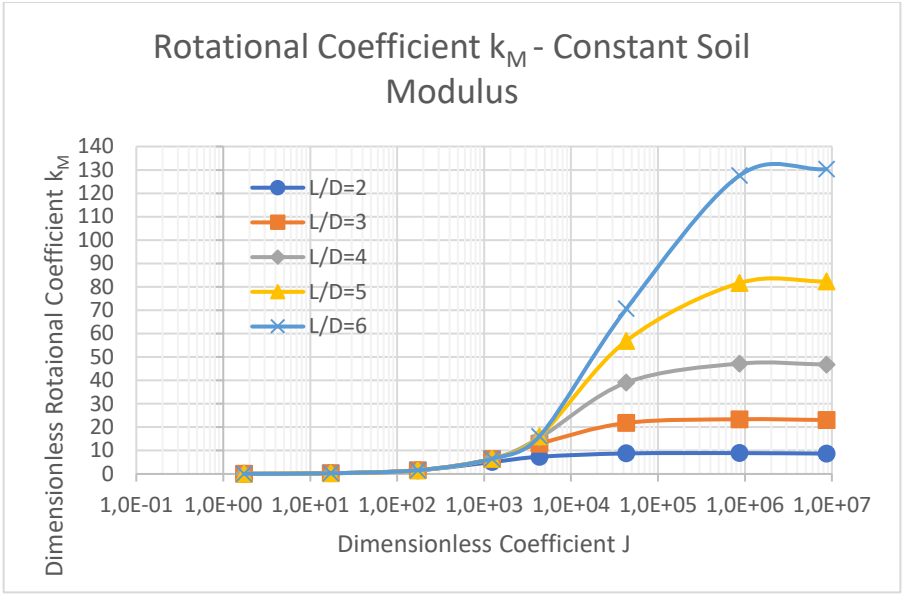

Figure 18: Normalized chart of the rotational stiffness

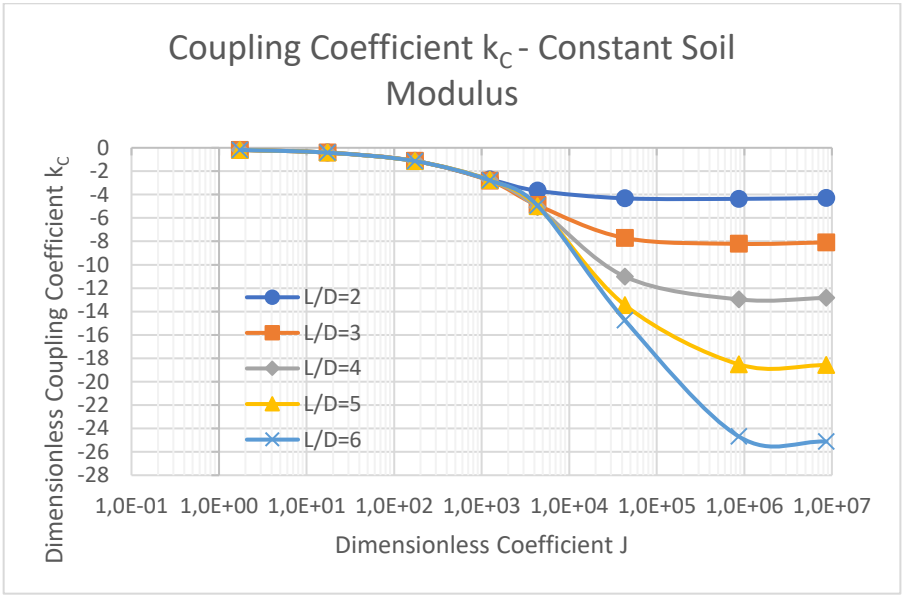

Figure 19: Normalized chart of the coupling stiffness

6.4 METHODOLOGY STEP BY STEP

This section gives a stepwise description of the procedure for determining the stiffness matrix for deflections at the monopile at seabed.

- The values of pile dimension and soil stiffness are known and inputs parameters in the procedure. The parameters give the ratio L/D
- From the equation (4.4) the soil profile it determined having the E_{ref} as known.
- The dimensionless coefficient J can be calculated by suing the equation (6.7)
- By using the charts, the dimensionless stiffness coefficients k_i is determined.
- Then multiply the formulas $(6.1 - 6.3)$ with the equivalent formulas $(6.4 - 6.6)$.
- Then solve for the Stiffness Coefficients K_i
- Finally, with the Stiffness Coefficients K_i, the formulas (2.13) and (2.14) can be solved to obtain the horizontal moment (u) and the inclination (θ).

6.5 EXAMPLES APPLICATION

Considering a monopile used for foundation type for an offshore wind turbine. It is assumed the diameter is 8m and length of the embedded pile 28m. The thickness is 0,1m (keeping the ratio D/t constant 80). The pile is founded in undrained normal consolidated clay which has a soil stiffness profile $E_s = 5\ 10^6\ z$, where E_s is in pascal and z in meters. The foundation is acquiring a horizontal moment of 4 MN in combination with an overturning moment of 120 MN m.

1. The reference elasticity modulus is calculated, $E_{ref} = 5 \times 10^6\ \times 8 = 4 \times 10^7\ Pa$.
2. Calculating the equivalent stiffness of the pile as $E_p^* = E_p \left(1 - \left(\frac{r-t}{r}\right)^4\right) = 1{,}93 \times 10^{10}\ Pa$. This gives the coefficient $J = \frac{E_p^*}{E_s}\left(\frac{L}{D}\right) = 1{,}7 \times 10^3$.

3. By using the charts for linear inhomogeneous soil modulus ($Figures\ 36-38$), the dimensionless coefficients are selected $k_F = 4.8$, $k_M = 10$ and $k_C = -5.5$.
4. Furthermore, the formulas $(6.1-6.3)$ are used with the correction factor (γ), formulas $(6.4-6.6)$:

   $K_F = k_F\, E_{ref}\, D\, \gamma_F = 4{,}8 \times 4 \times 10^7 \times 8 \times 1{,}5 \times (28/8)^{-0{,}16} = 1{,}89 \times 10^9\ Pa\ m.$

The same procedure takes place for the other two coefficients. In more detail:

$K_M = k_M\, E_{ref}\, D\, \gamma_M = 10 \times 4 \times 10^7 \times 8 \times 4{,}73 \times (28/8)^{-0{,}66} = 4{,}24\ 10^{11}\ Pa\ m^3$

$K_C = k_C\, E_{ref}\, D\, \gamma_C = -5{,}5 \times 4 \times 10^7 \times 8 \times 2{,}78 \times (28/8)^{-0{,}43} = -2{,}28\ 10^{10}\ Pa\ m^2.$

5. Now by using the equation for the deflection (2.13) and (2.14) the results are, for the displacement $u = 0{,}016\ m$ and for the inclination $\theta = 1{,}13 \times 10^{-3}\ rad$ or $\theta = 0{,}065°$

Finally, the results of the stiffness coefficient for each direction along with coupling term, was compared with the result form the PILES program. The results are found to agree very well:

Table 26: Comparison f the results between charts and PILES program

	K_F [Pa m]	K_M [Pa m³]	K_C [Pa m²]
Charts	1,89E+09	4,24E+11	-2,28E+10
PILES	2,03E+09	4,46E+11	-2,30E+10
Accuracy (%)	93,1	95,1	98,2

7 CONCLUSION AND FURTHER WORK

7.1 SUMMARY AND CONCLUSION

In this thesis, a methodology was proposed to calculate the stiffness coeffects of an offshore monopile foundation when lateral load a bending moment is applied. The purpose was to calculate fast and accurate the stiffness of the system soil/pile in order to calculate the deflection at the pile head of the foundation. The study has focused on the gap between the response of a rigid and flexible pile is very important.

This methodology was created based on the results from the NGI's in-house program PILES and the FE program PLAXIS 3D.

It was shown that the well-established formulas from Gazetas and Shadlou represented the upper and lower boundaries of the study.

At high slenderness ratio of the results in the study were approaching 93% comparing the ones from PLAXIS. At low slenderness ratio, the results in the study were approaching 98% comparing the ones from PLAXIS

Finally, after sensitive study for several case studies with, variations in soil conditions, they were normalized and presented in charts. Concluding, the charts have the potential to calculate the horizontal, moment and coupling term of the stiffness coefficient efficiently. These coefficients then can be used to calculate the deflections which are necessary for a safe an inexpensive foundation design.

7.2 RECOMMENDATIONS FOR FURTHER WORK

This master thesis has proposed a methodology to calculate the static stiffness coefficient at the pile head of a monopile foundation. There were some limitations for this project which can be an additional feature in the future. Therefore, this method is not valid for the following condition and they can be a recommendation for further work:

- A different ratio of diameter over the wall thickness (D/t) which was kept constant at the value 80 for the whole study.
- This method is only valid for undrained soil conditions. Thus, a similar study for drained condition can be considered in the future.

- Apart from the load cases of horizontal load and bending moment, a vertical load and torsion can be studied in a similar way.
- The state of loading was static, therefore the effect of cyclic and for dynamic loading has not studied. A similar method for these kinds of loadings will be extremely helpful more accurate design of monopiles.

REFERENCES

Abed, Y., Bouzid, D. A., Bhattacharya, S., & Aissa, M. H. (2016). Static impedance functions for monopiles supporting offshore wind turbines in nonhomogeneous soils-emphasis on soil/monopile interface characteristics. *Earthquakes and Structures, 10*(5), 1143-1179.

Adhikari, S., & Bhattacharya, S. (2011). Vibrations of wind-turbines considering soil-structure interaction. *Wind and Structures, 14*(2), 85.

Adhikari, S., & Bhattacharya, S. (2012). Dynamic analysis of wind turbine towers on flexible foundations. *Shock and vibration, 19*(1), 37-56.

API. (2011). API RP2 GEO: Specific requirements for offshore structures, geotechnical and foundation design considerations. In *American Petroleum Institute*.

Arany, L., Bhattacharya, S., Adhikari, S., Hogan, S., & Macdonald, J. (2015). An analytical model to predict the natural frequency of offshore wind turbines on three-spring flexible foundations using two different beam models. *Soil Dynamics and Earthquake Engineering, 74*, 40-45.

Baguelin, F., Frank, R., & Said, Y. (1977). Theoretical study of lateral reaction mechanism of piles. *Geotechnique, 27*(3), 405-434.

Barber, E. (1953). Discussion to paper by SM Gleser. *ASTM, STP, 154*, 96-99.

Basu, D., Salgado, R., & Prezzi, M. (2008). Analysis of laterally loaded piles in multilayered soil deposits.

Biot, M. (1922). Bending of an infinite beam on an elastic foundation. *Journal of Applied Mathematics and Mechanics, 2*(3), 165-184.

Byrne, B., McAdam, R., Burd, H., Houlsby, G., Martin, C., Gavin, K., . . . Taborda, D. (2015b). Field testing of large diameter piles under lateral loading for offshore wind applications. In.

Byrne, B., McAdam, R., Burd, H., Houlsby, G., Martin, C., Zdravković, L., . . . Sideri, M. (2015a). *New design methods for large diameter piles under lateral loading for offshore wind applications.* Paper presented at the 3rd International Symposium on Frontiers in Offshore Geotechnics (ISFOG 2015), Oslo, Norway, June.

Damgaard, M., Zania, V., Andersen, L. V., & Ibsen, L. B. (2014). Effects of soil–structure interaction on real time dynamic response of offshore wind turbines on monopiles. *Engineering Structures, 75*, 388-401.

Doherty, J., Houlsby, G., & Deeks, A. (2005). Stiffness of flexible caisson foundations embedded in nonhomogeneous elastic soil. *Journal of*

geotechnical and geoenvironmental engineering, 131(12), 1498-1508.
Doherty, J. P., & Deeks, A. J. (2003). Scaled boundary finite-element analysis of a non-homogeneous axisymmetric domain subjected to general loading. *International journal for numerical and analytical methods in geomechanics, 27*(10), 813-835.
Europe, W. (2017). The European offshore wind industry—Key trends and statistics 2016. *Wind Europe: Brussels, Belgium*, 37.
Gazetas, G. (1984). Seismic response of end-bearing single piles. *International Journal of Soil Dynamics and Earthquake Engineering, 3*(2), 82-93.
Gazetas, G. (1991). Foundation vibrations. In *Foundation engineering handbook* (pp. 553-593): Springer.
Gupta, B. K., & Basu, D. (2016). Analysis of laterally loaded rigid monopiles and poles in multilayered linearly varying soil. *Computers and Geotechnics, 72*, 114-125.
Hanssen, S. B. (2016). Response of laterally loaded monopiles.
Hetenyi, M. (1946). Beams on elastic foundation. *Ann Arbor: University of Michigan Press*.
IRENA. (2018). Renewable capacity statistics 2018. *International Renewable Energy Agency (IRENA), Abu Dhabi*.
Kallehave, D., Byrne, B. W., Thilsted, C. L., & Mikkelsen, K. K. (2015). Optimization of monopiles for offshore wind turbines. *Phil. Trans. R. Soc. A, 373*(2035), 20140100.
Kallehave, D., Thilsted, C. L., & Liingaard, M. (2012). *Modification of the API py formulation of initial stiffness of sand.* Paper presented at the Offshore site investigation and geotechnics: integrated technologies-present and future.
Kaynia, A. M., & Kausel, E. (1991). Dynamics of piles and pile groups in layered soil media. *Soil Dynamics and Earthquake Engineering, 10*(8), 386-401.
Lombardi, D., Bhattacharya, S., & Wood, D. M. (2013). Dynamic soil–structure interaction of monopile supported wind turbines in cohesive soil. *Soil Dynamics and Earthquake Engineering, 49*, 165-180.
Matlock, H. (1970). Correlations for design of laterally loaded piles in soft clay. *Offshore Technology in Civil Engineering Hall of Fame Papers from the Early Years*, 77-94.
Mukherjee, S., & Dey, A. (2016). Analysis Of Laterally Loaded Fixed Headed Single Floating Pile In Multilayered Soil Using Bef Approach.
O'Neill, M. W., & Murchison, J. M. (1983). *An evaluation of p-y relationships in sands*: University of Houston.

Pender, M. (1993). Aseismic pile foundation design analysis. *Bulletin of the New Zealand National Society for Earthquake Engrg, 26*(1), 49-160.

Poulos, H. G., & Davis, E. H. (1980). *Pile foundation analysis and design*.

Randolph, M. F. (1981). The response of flexible piles to lateral loading. *Geotechnique, 31*(2), 247-259.

Reese, L. C., Cox, W. R., & Koop, F. D. (1975). *Field testing and analysis of laterally loaded piles om stiff clay.* Paper presented at the Offshore Technology Conference.

Shadlou, M., & Bhattacharya, S. (2016). Dynamic stiffness of monopiles supporting offshore wind turbine generators. *Soil Dynamics and Earthquake Engineering, 88*, 15-32.

Steinar, N. (2017). *Geotechnical Engineering Advance Course*.

Veritas, D. N. (2004). Design of Offshore Wind Turbine Structure. *Offshore Standard DNV-OS-J101*.

Winkler, E. (1867). *Die Lehre von der Elasticitaet und Festigkeit: mit besonderer Rücksicht auf ihre Anwendung in der Technik für polytechnische Schulen, Bauakademien, Ingenieue, Maschinenbauer, Architecten, etc* (Vol. 1): Dominicus.

Wolf, J. P., & Song, C. (1996). *Finite-element modelling of unbounded media*: Wiley Chichester.

Zaaijer, M. (2006). Foundation modelling to assess dynamic behaviour of offshore wind turbines. *Applied Ocean Research, 28*(1), 45-57.

Zania, V. (2014). Natural vibration frequency and damping of slender structures founded on monopiles. *Soil Dynamics and Earthquake Engineering, 59*, 8-20.

Zdravković, L., Taborda, D., Potts, D., Jardine, R., Sideri, M., Schroeder, F., . . . Houlsby, G. (2015). *Numerical modelling of large diameter piles under lateral loading for offshore wind applications.* Paper presented at the Proceeding 3rd International Symposium on Frontiers in Offshore Geotechnics. Norway:[sn].

NOMENCLATURE

D	diameter
E	Young's modulus
EA	axial stiffness
EI	bending stiffness
E_p	Young's modulus of the pile
E_p^*	relative Young's modulus of the pile
E_{ref}	Young's modulus at depth of one diameter
E_s	Young's modulus of the soil
F	load
F_h	horizontal load
G	shear modulus
K_C	coupling stiffness
K_F	horizontal stiffness
K_M	rotational stiffness
L	pile length
l_c	active length of the pile
M	bending moment
p(y)	lateral deflection
Q_A	axial force
Q_C	lateral force
t	thickness of the pile wall
u	lateral displacement
v_s	shear wave velocity
y	lateral displacement

z	depth from the mudline level
γ	unit weight
ε	strain
θ	inclination of the pile head
ν	Poisson's ratio
ρ	density
σ	stress

LIST OF FIGURES

LIST OF TABLES

APPENDIX

Table 27: Stiffness coefficients for slender pile in medium homogeneous soil

Stiffness Coefficients		
[Slender] (Gazetas, 1984)		
Horizontal	Rotation	Coupling
K_F [Pa m]	K_M [Pa m^3]	K_C [Pa m^2]
1,42E+09	4,80E+11	-1,56E+10

Table 28: Stiffness coefficients for rigid pile in medium homogeneous soil

Stiffness Coefficients			
[Rigid] (Shadlou & Bhattacharya, 2016)			
Length	Horizontal	Rotation	Coupling
L [m]	K_F [Pa m]	K_M [Pa m^3]	K_C [Pa m^2]
18	1,42E+09	2,19E+11	-1,30E+10
27	1,83E+09	6,02E+11	-2,46E+10
36	2,19E+09	1,24E+12	-3,85E+10
45	2,51E+09	2,16E+12	-5,45E+10
54	2,81E+09	3,41E+12	-7,24E+10

Table 29: Stiffness coefficients for slender pile in stiff homogeneous soil

Stiffness Coefficients		
[Slender] (Gazetas, 1984)		
Horizontal	Rotation	Coupling
K_F [Pa m]	K_M [Pa m^3]	K_C [Pa m^2]
3,83E+09	6,56E+11	-2,93E+10

Table 30: Stiffness coefficients for rigid pile in stiff homogeneous soil

Stiffness Coefficients			
[Rigid] (Shadlou & Bhattacharya, 2016)			
Length	Horizontal	Rotation	Coupling
L [m]	K_F [Pa m]	K_M [Pa m^3]	K_C [Pa m^2]
18	4,98E+09	7,65E+11	-4,57E+10
27	6,40E+09	2,11E+12	-8,59E+10
36	7,65E+09	4,33E+12	-1,35E+11
45	8,78E+09	7,56E+12	-1,91E+11
54	9,84E+09	1,19E+13	-2,53E+11

Table 31: Stiffness coefficients for slender pile in linear nonhomogeneous soil

Stiffness Coefficients		
[Slender] (Gazetas, 1984)		
Horizontal	Rotation	Coupling
K_F [Pa m]	K_M [Pa m^3]	K_C [Pa m^2]
4,20E+08	3,61E+11	-8,92E+09

Table 32: Stiffness coefficients for rigid pile in linear nonhomogeneous soil

Stiffness Coefficients			
[Rigid] (Shadlou & Bhattacharya, 2016)			
Length	Horizontal	Rotation	Coupling
L [m]	K_F [Pa m]	K_M [Pa m^3]	K_C [Pa m^2]
18	1,96E+08	4,04E+10	-2,61E+09
27	3,65E+08	1,64E+11	-7,20E+09
36	5,67E+08	4,42E+11	-1,48E+10
45	7,97E+08	9,54E+11	-2,58E+10
54	1,05E+09	1,79E+12	-4,07E+10

Table 33: Stiffness coefficients for slender pile in parabolic nonhomogeneous soil

Stiffness Coefficients		
[Slender] (Gazetas, 1984)		
Horizontal	Rotation	Coupling
K_F [Pa m]	K_M [Pa m^3]	K_C [Pa m^2]
3,06E+08	3,00E+11	-6,96E+09

Table 34: Stiffness coefficients for rigid pile in parabolic nonhomogeneous soil

Stiffness Coefficients			
[Rigid] (Shadlou & Bhattacharya, 2016)			
Length	Horizontal	Rotation	Coupling
L [m]	K_F [Pa m]	K_M [Pa m^3]	K_C [Pa m^2]
18	1,61E+08	3,05E+10	-1,87E+09
27	2,49E+08	1,03E+11	-4,22E+09
36	3,39E+08	2,44E+11	-7,49E+09
45	4,30E+08	4,77E+11	-1,17E+10
54	5,23E+08	8,25E+11	-1,69E+10

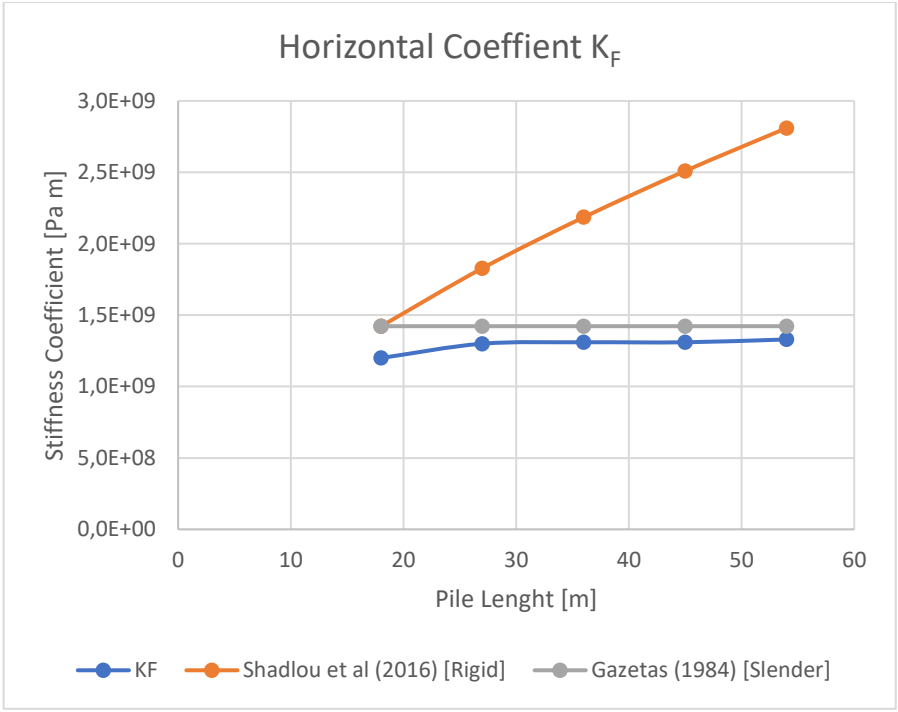

Figure 20: Results of horizontal stiffness change by pile length for homogeneous medium soil

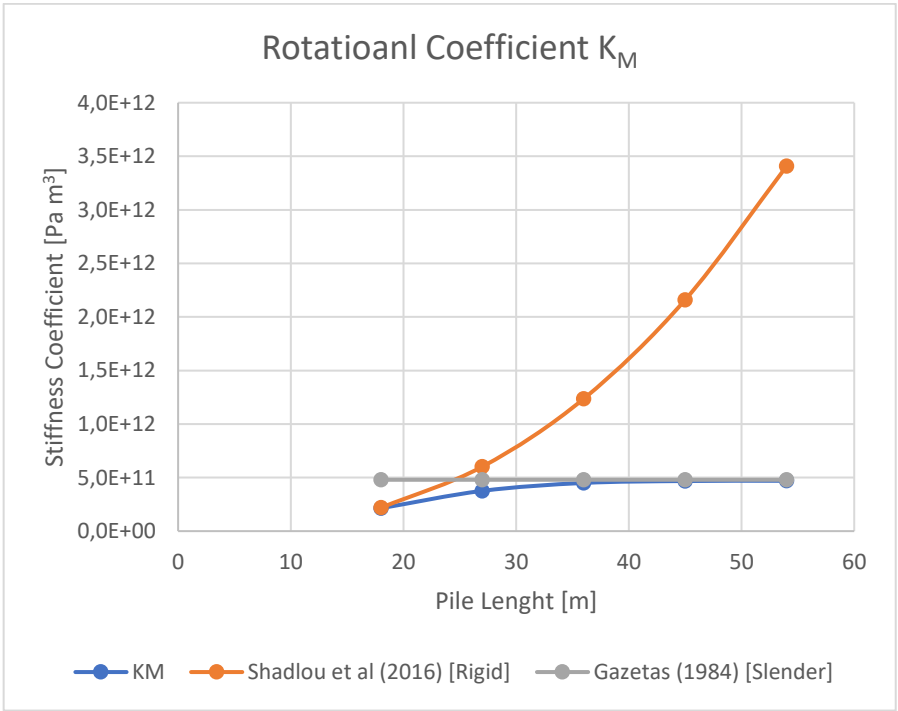

Figure 21: Results of rotational stiffness change by pile length for homogeneous medium soil

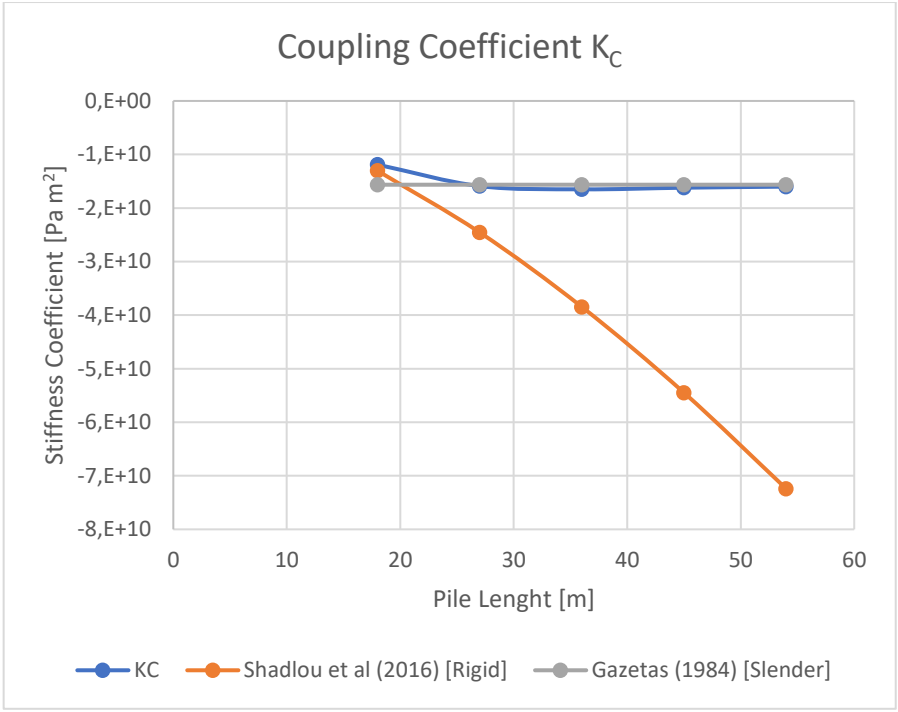

Figure 22: Results of coupling stiffness change by pile length for homogeneous medium soil

Figure 23: Results of horizontal stiffness change by pile length for homogeneous stiff soil

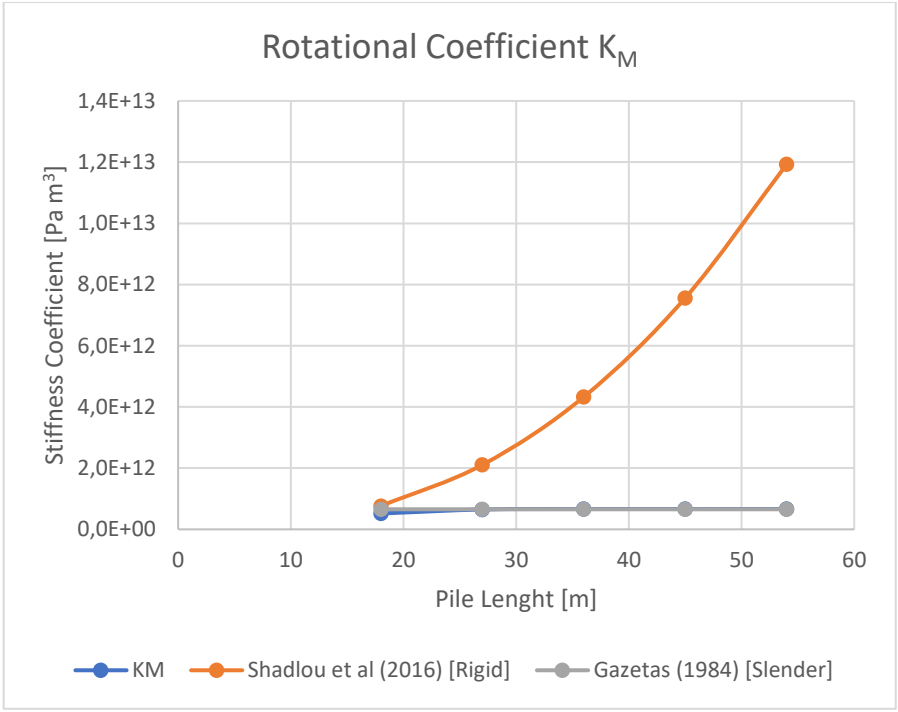

Figure 24: Results of rotational stiffness change by pile length for homogeneous stiff soil

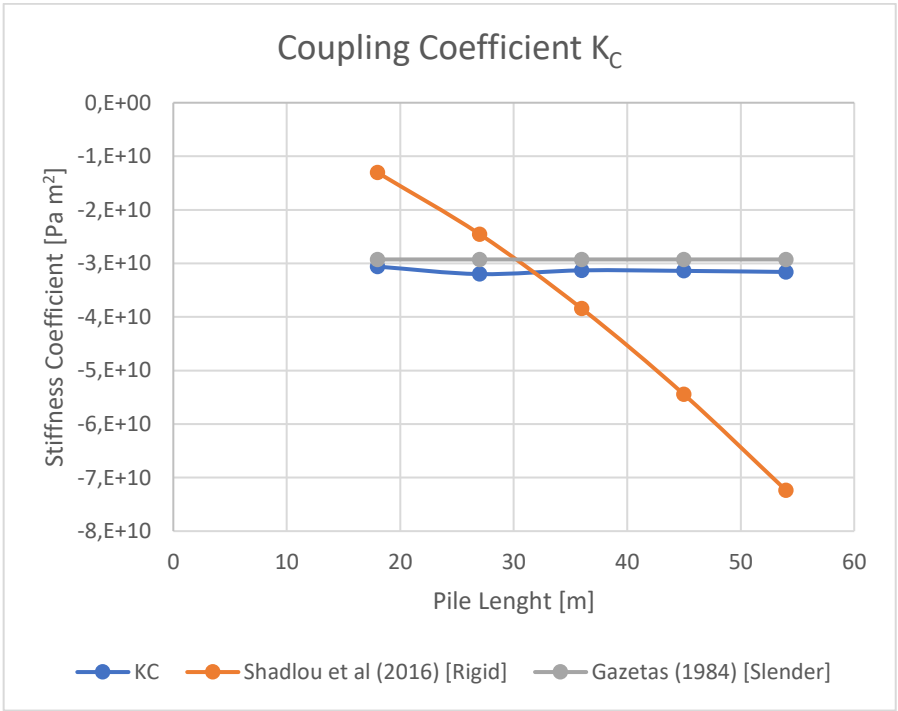

Figure 25: Results of coupling stiffness change by pile length for homogeneous stiff soil

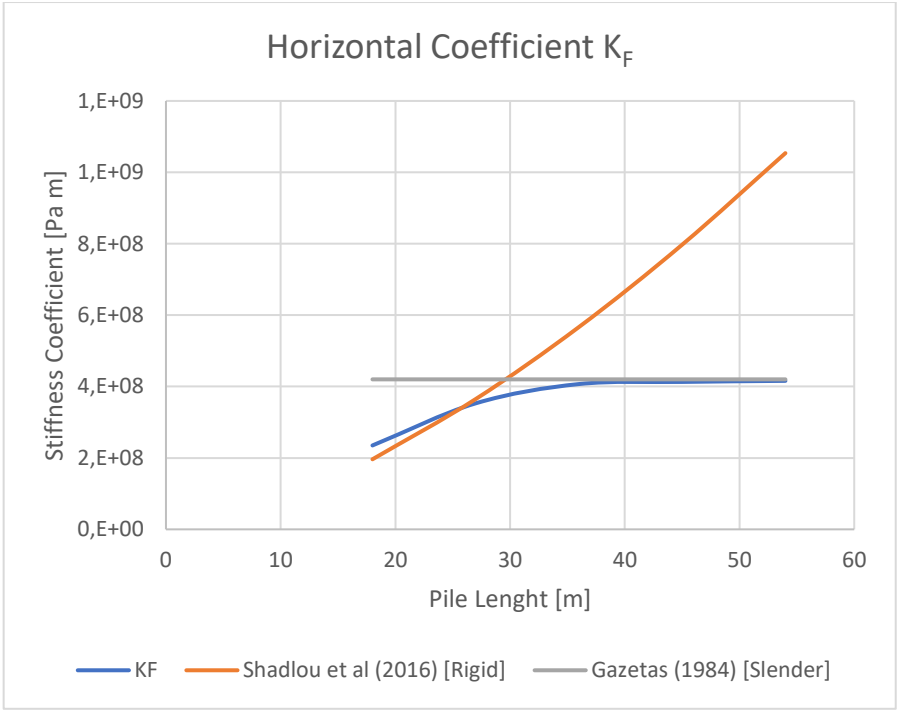

Figure 26: Results of horizontal stiffness change by pile length for linear nonhomogeneous soil

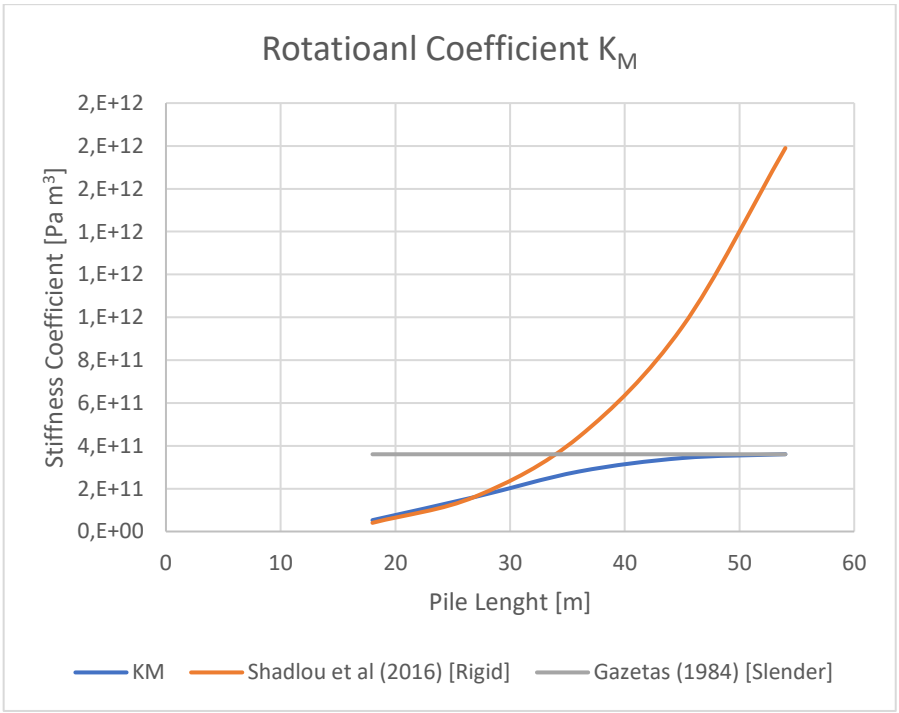

Figure 27: Results of rotational stiffness change by pile length for linear nonhomogeneous soil

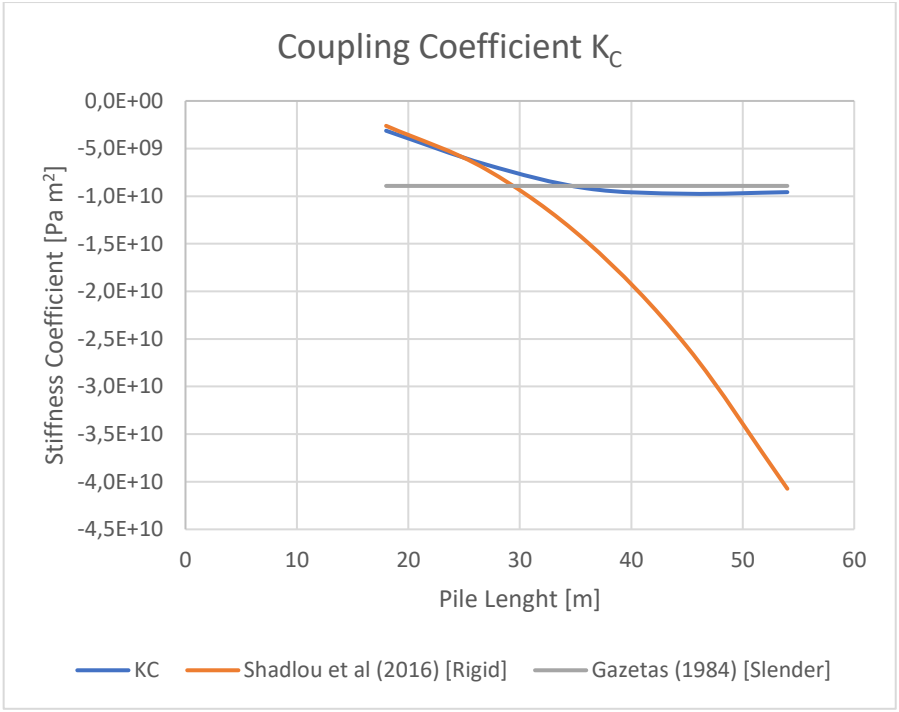

Figure 28: Results of coupling stiffness change by pile length for linear nonhomogeneous soil

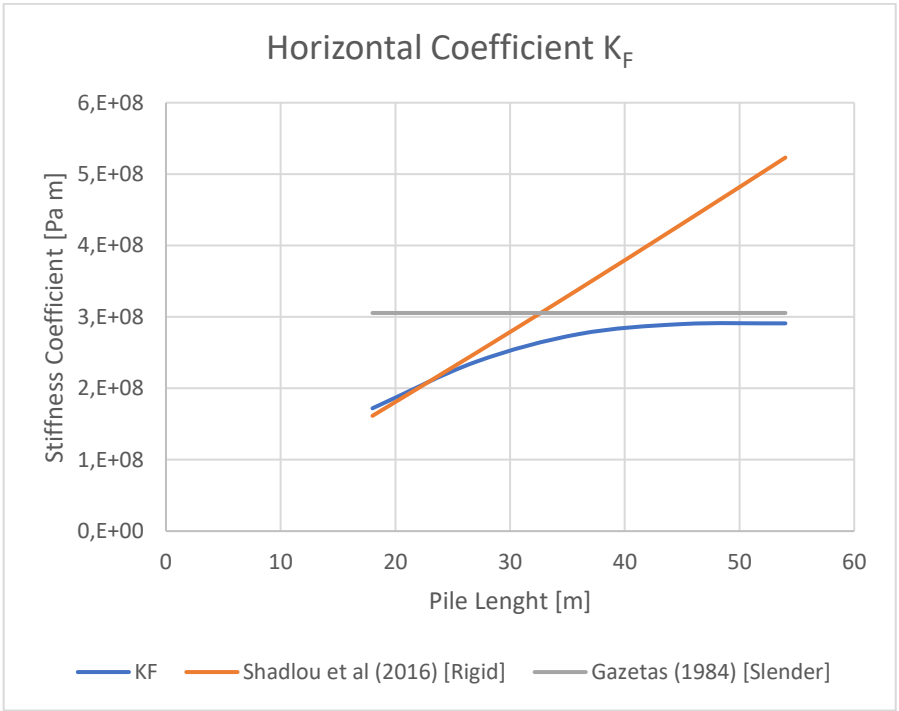

Figure 29: Results of horizontal stiffness change by pile length for parabolic nonhomogeneous soil

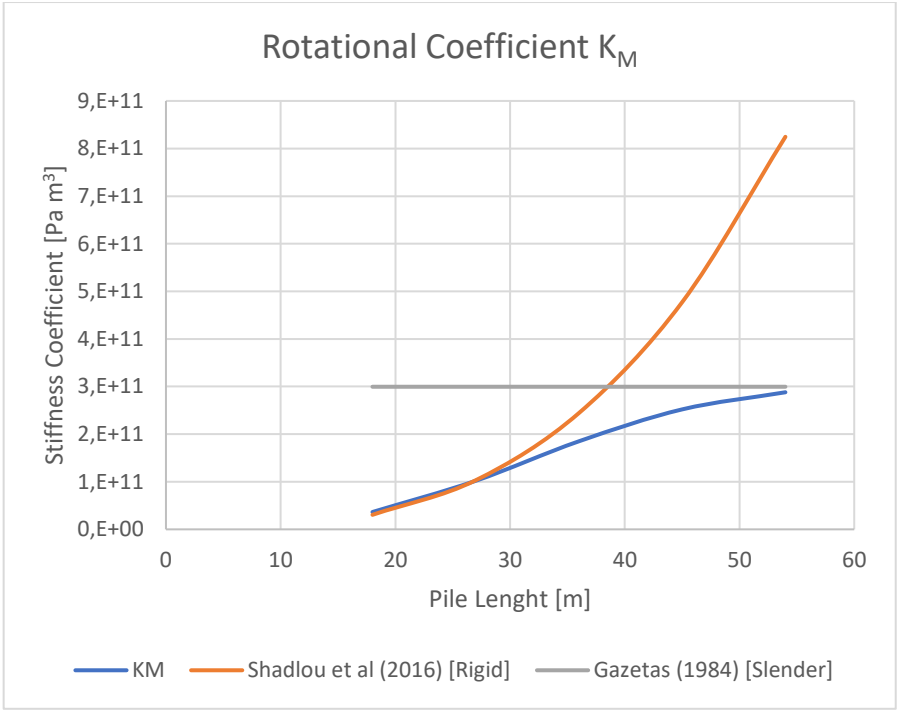

Figure 30: Results of rotational stiffness change by pile length for parabolic nonhomogeneous soil

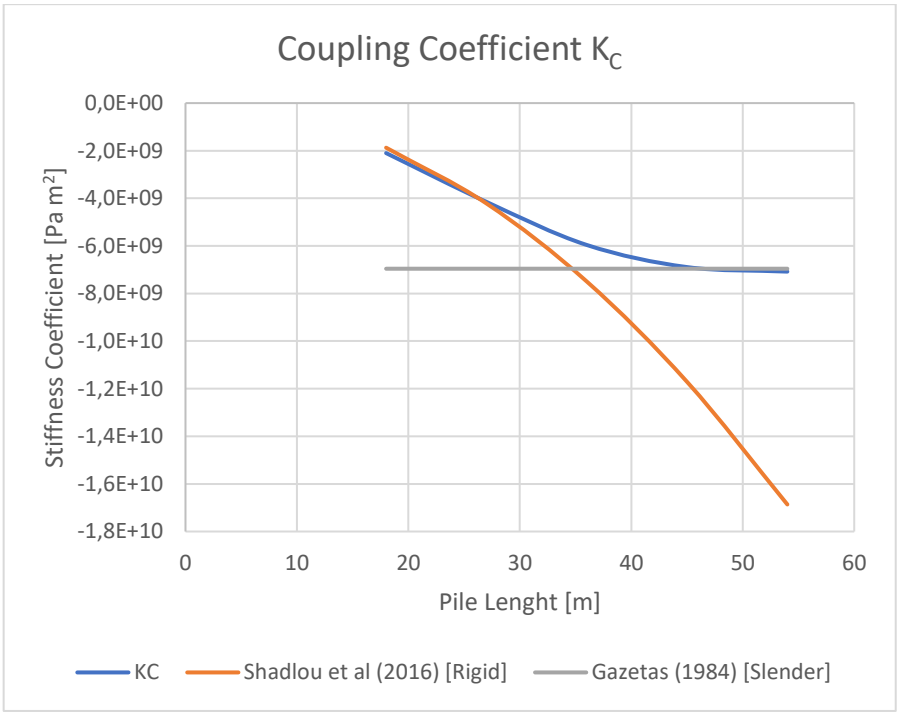

Figure 31: Results of coupling stiffness change by pile length for parabolic nonhomogeneous soil

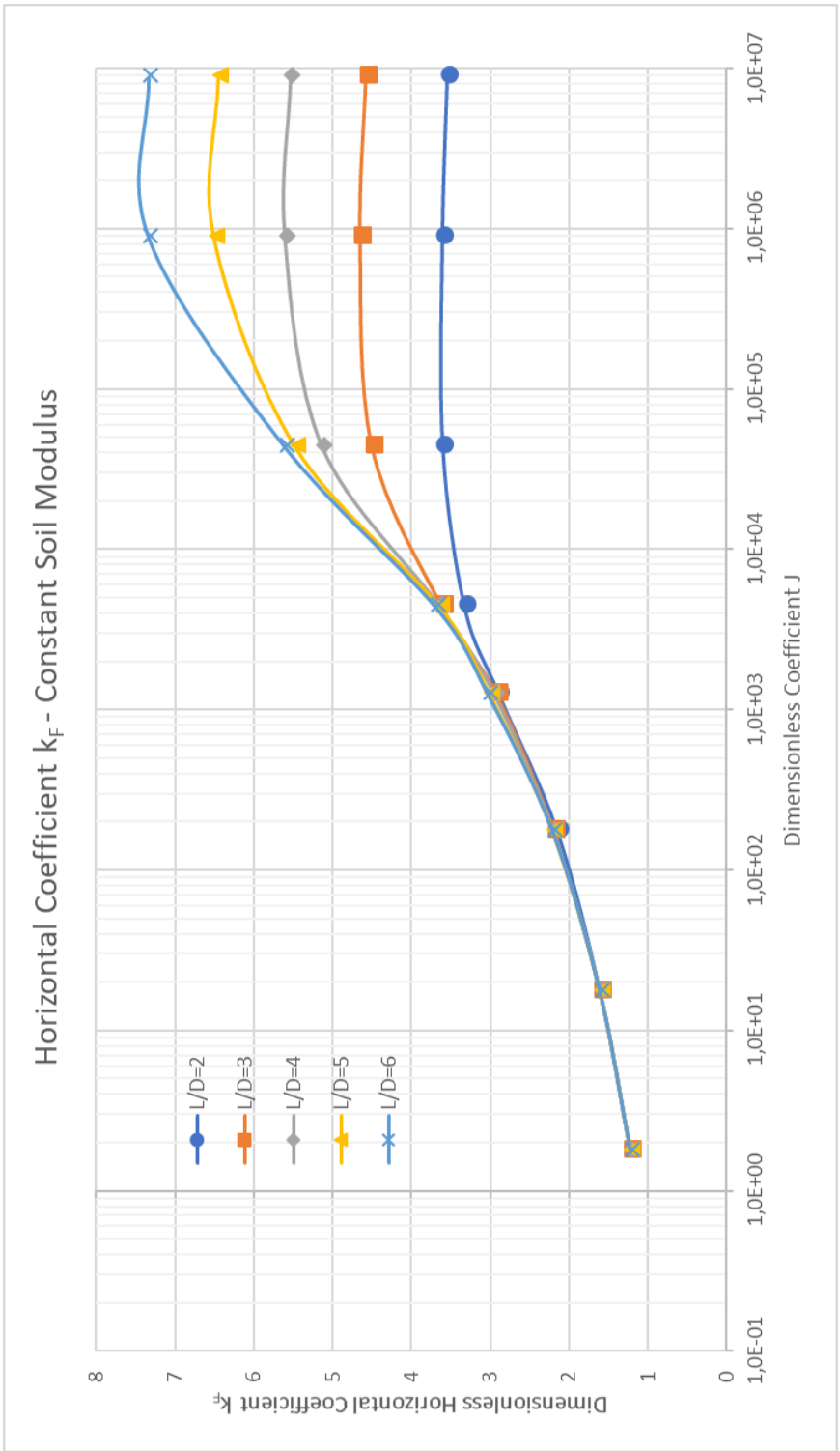

Figure 32: Normalized chart of the horizontal stiffness in homogeneous soil

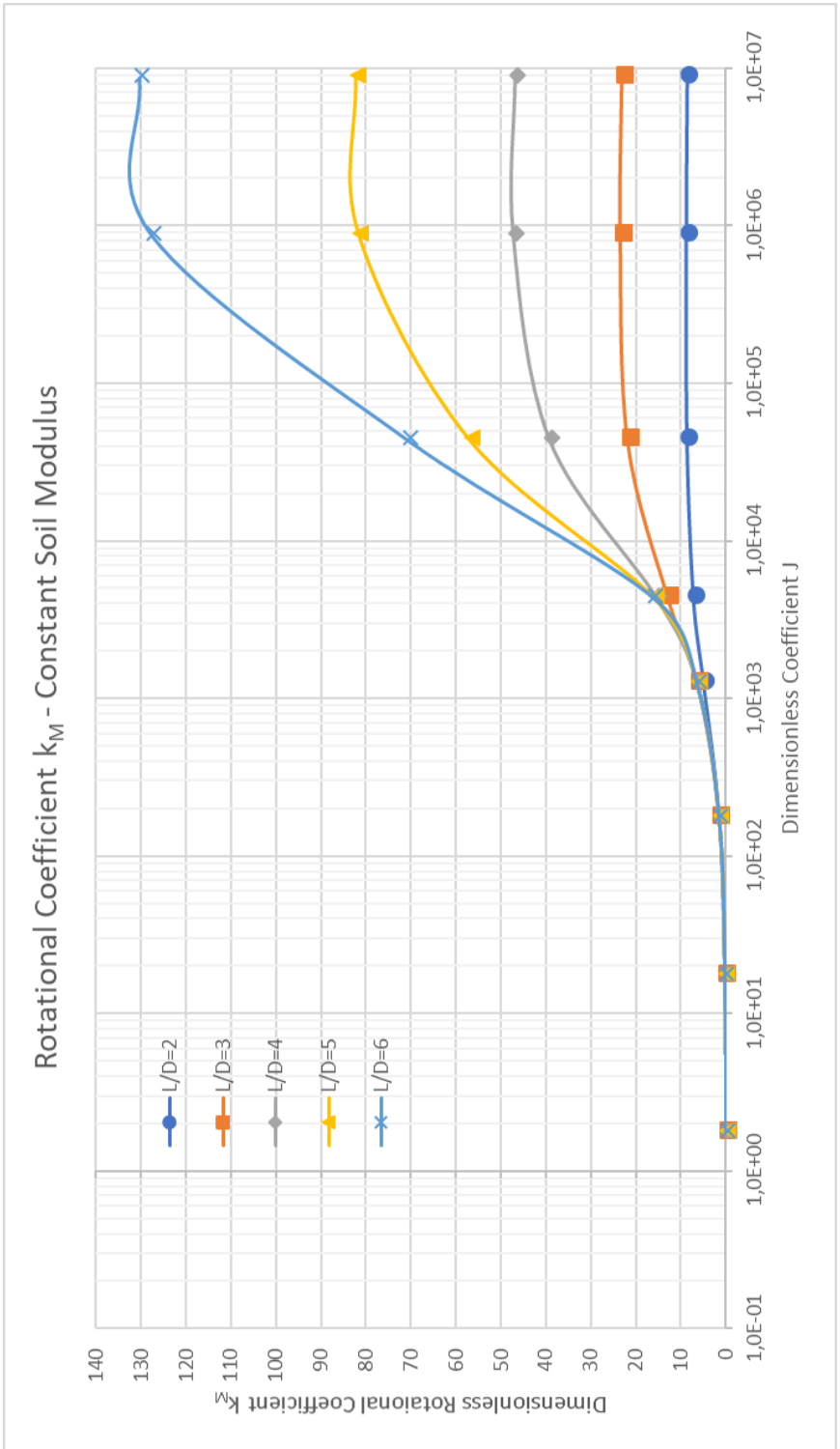

Figure 33: Normalized chart of the rotational stiffness in homogeneous soil

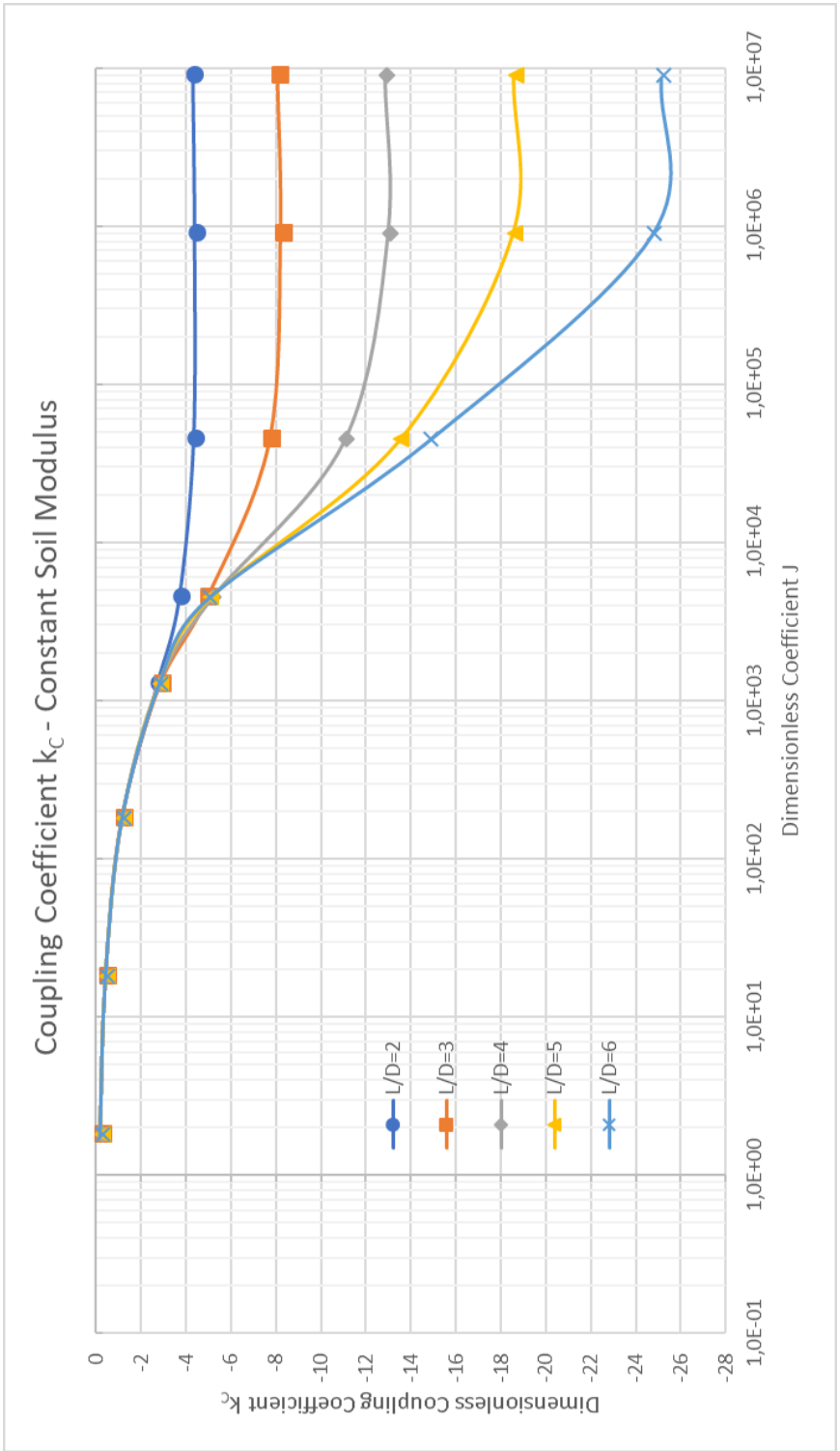

Figure 34: Normalized chart of the coupling stiffness in homogeneous soil

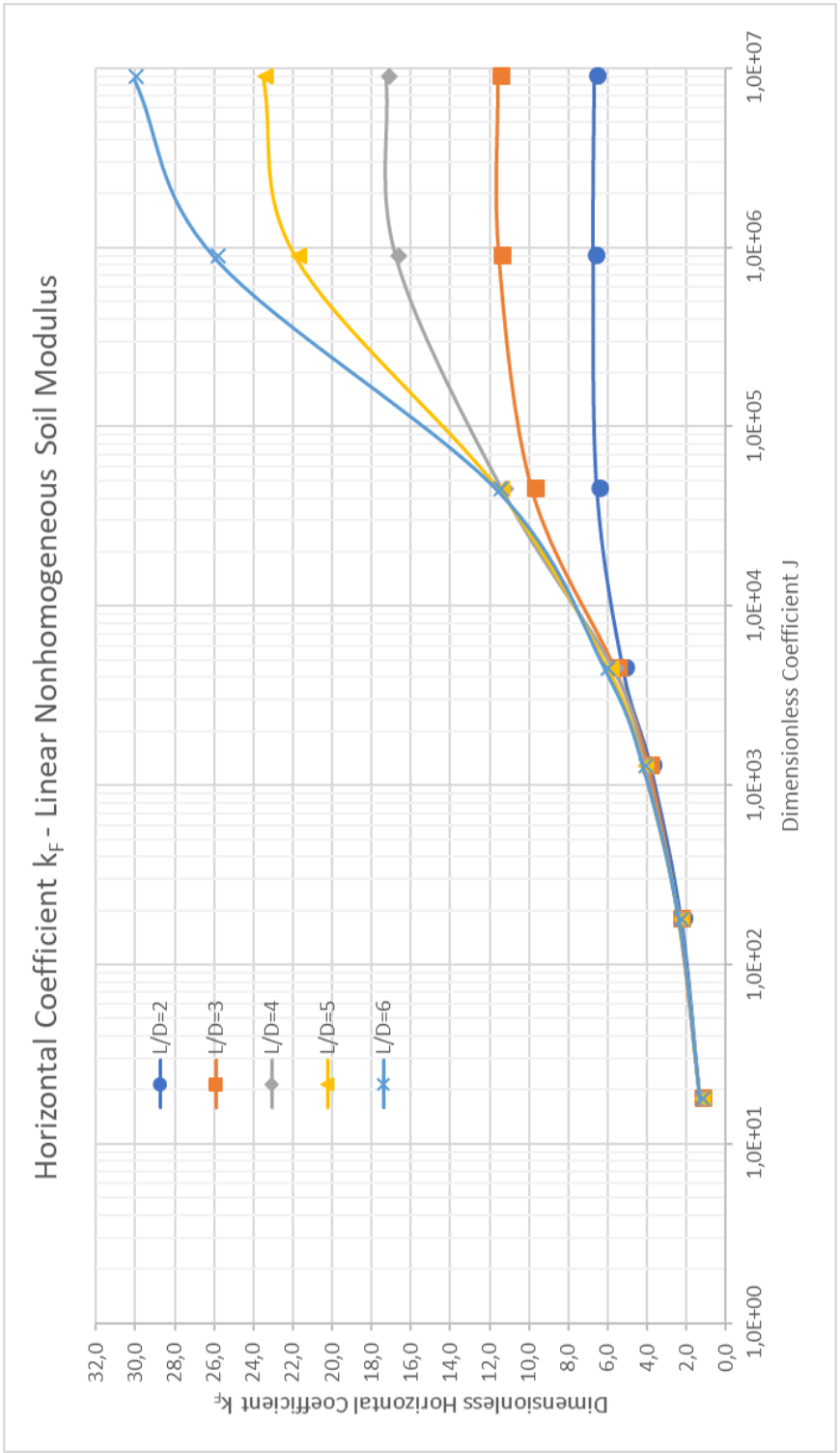

Figure 35: Normalized chart of the horizontal stiffness in linear nonhomogeneous soil

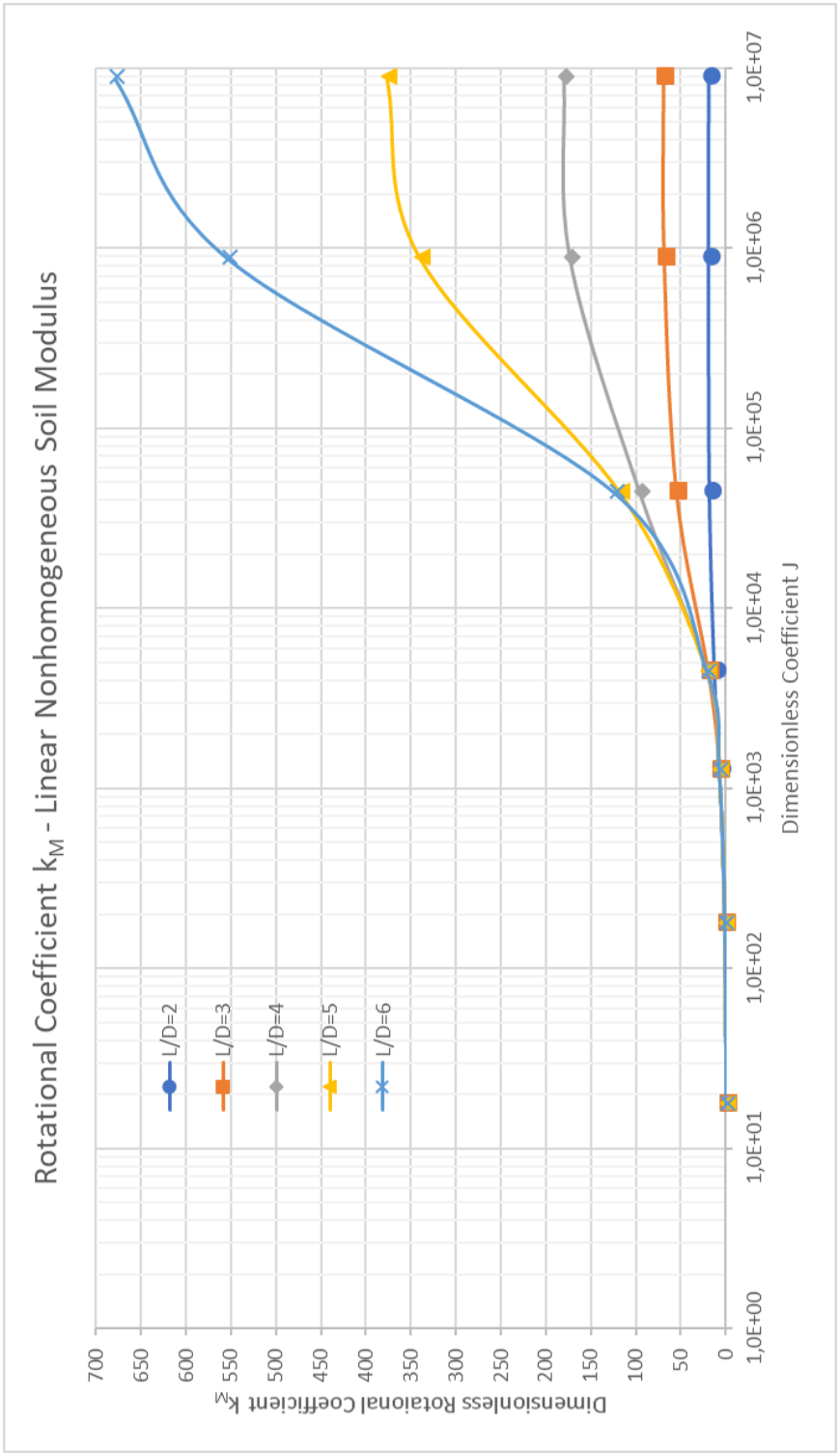

Figure 36: Normalized chart of the rotational stiffness in linear nonhomogeneous soil

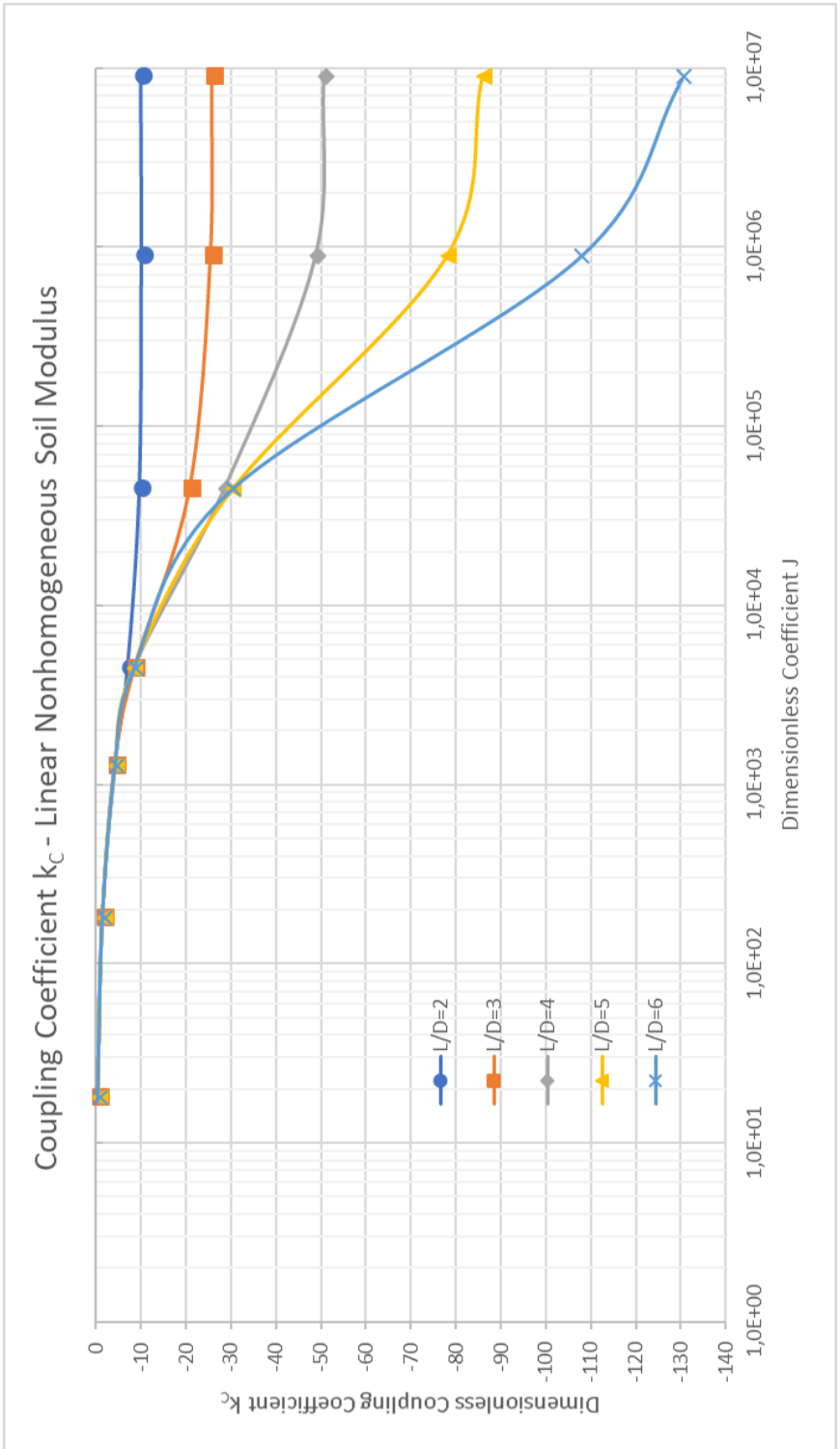

Figure 37: Normalized chart of the coupling stiffness in linear nonhomogeneous soil

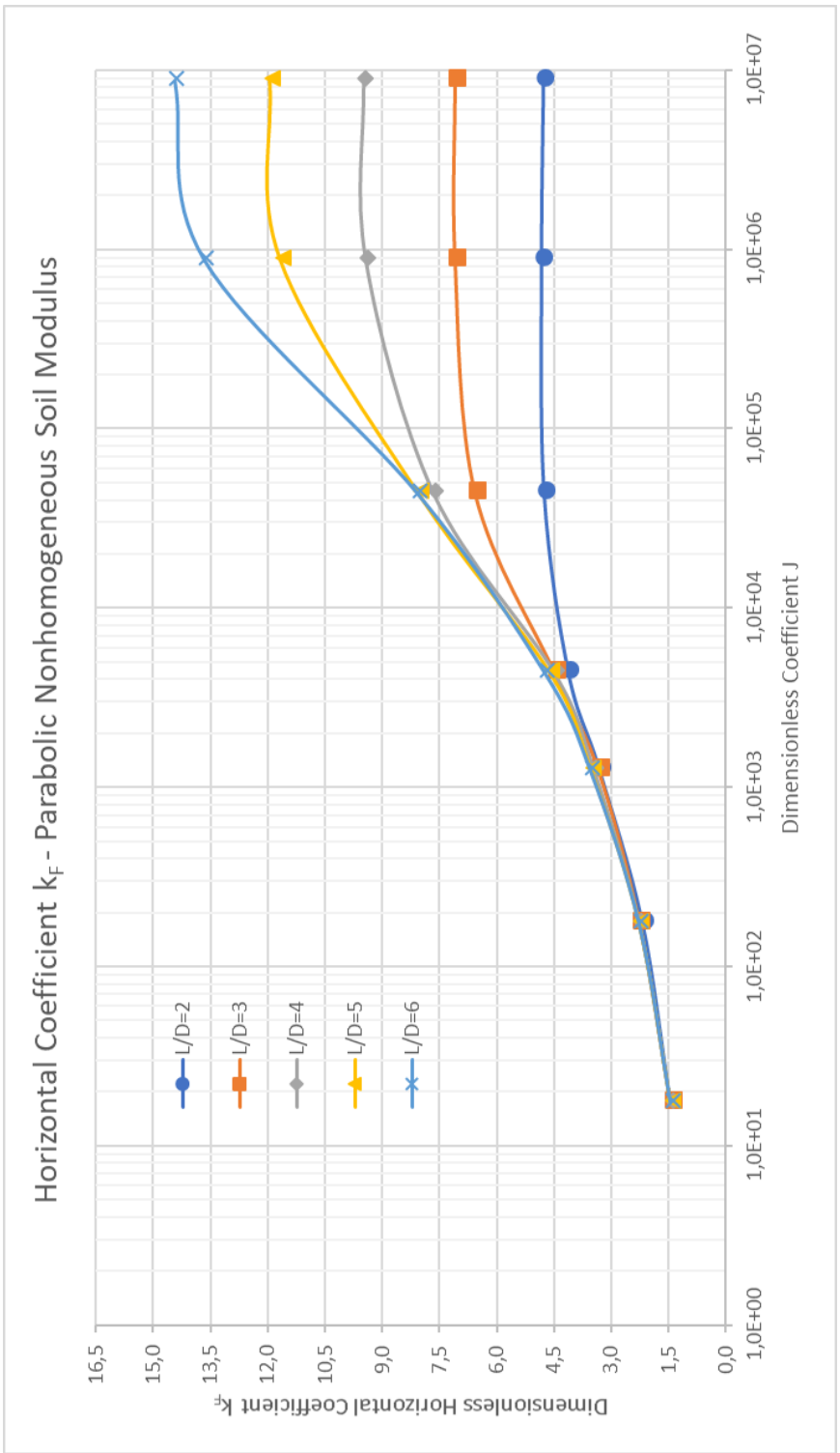

Figure 38: Normalized chart of the horizontal stiffness in parabolic nonhomogeneous soil

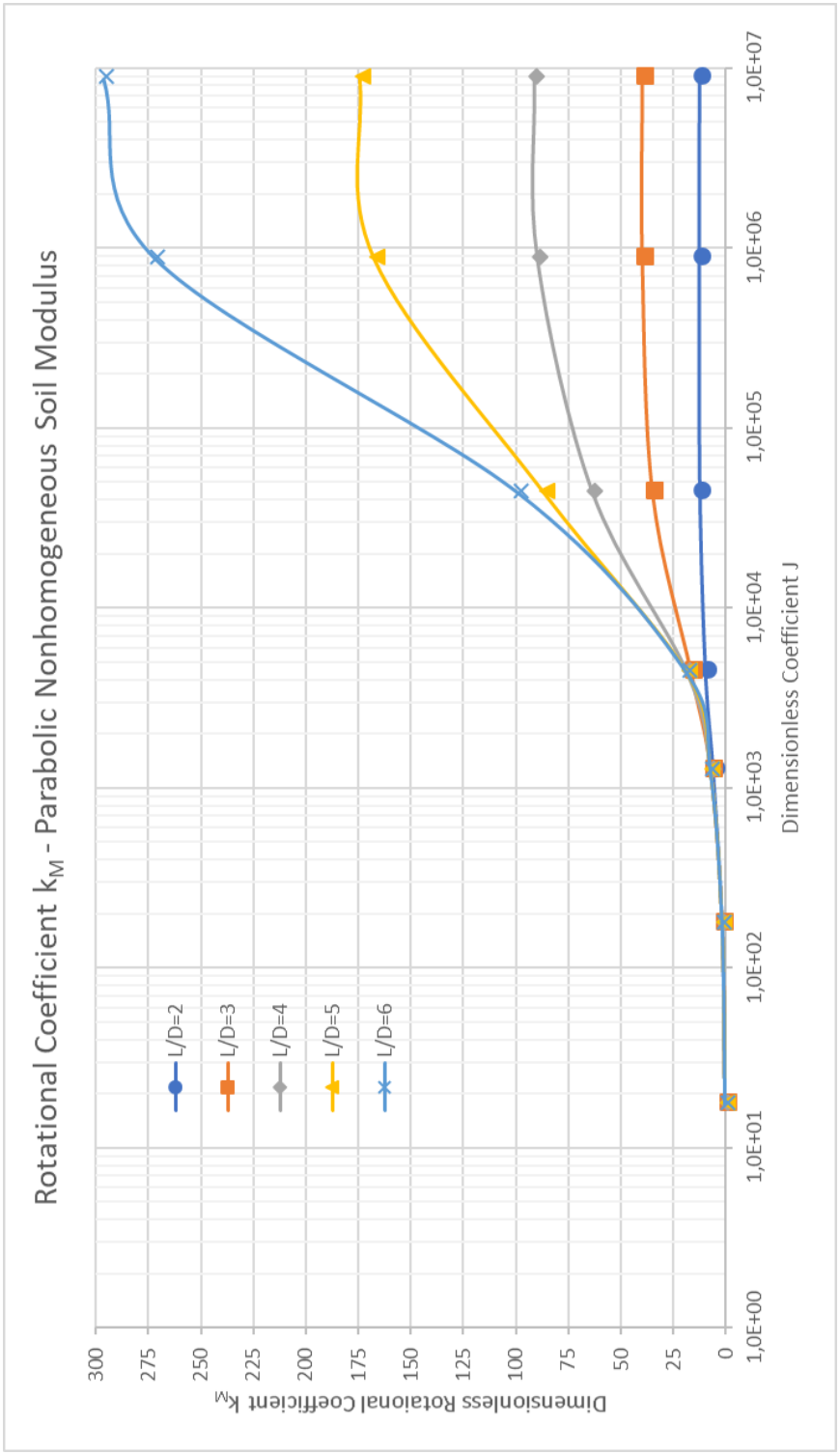

Figure 39: Normalized chart of the rotational stiffness in parabolic nonhomogeneous soil

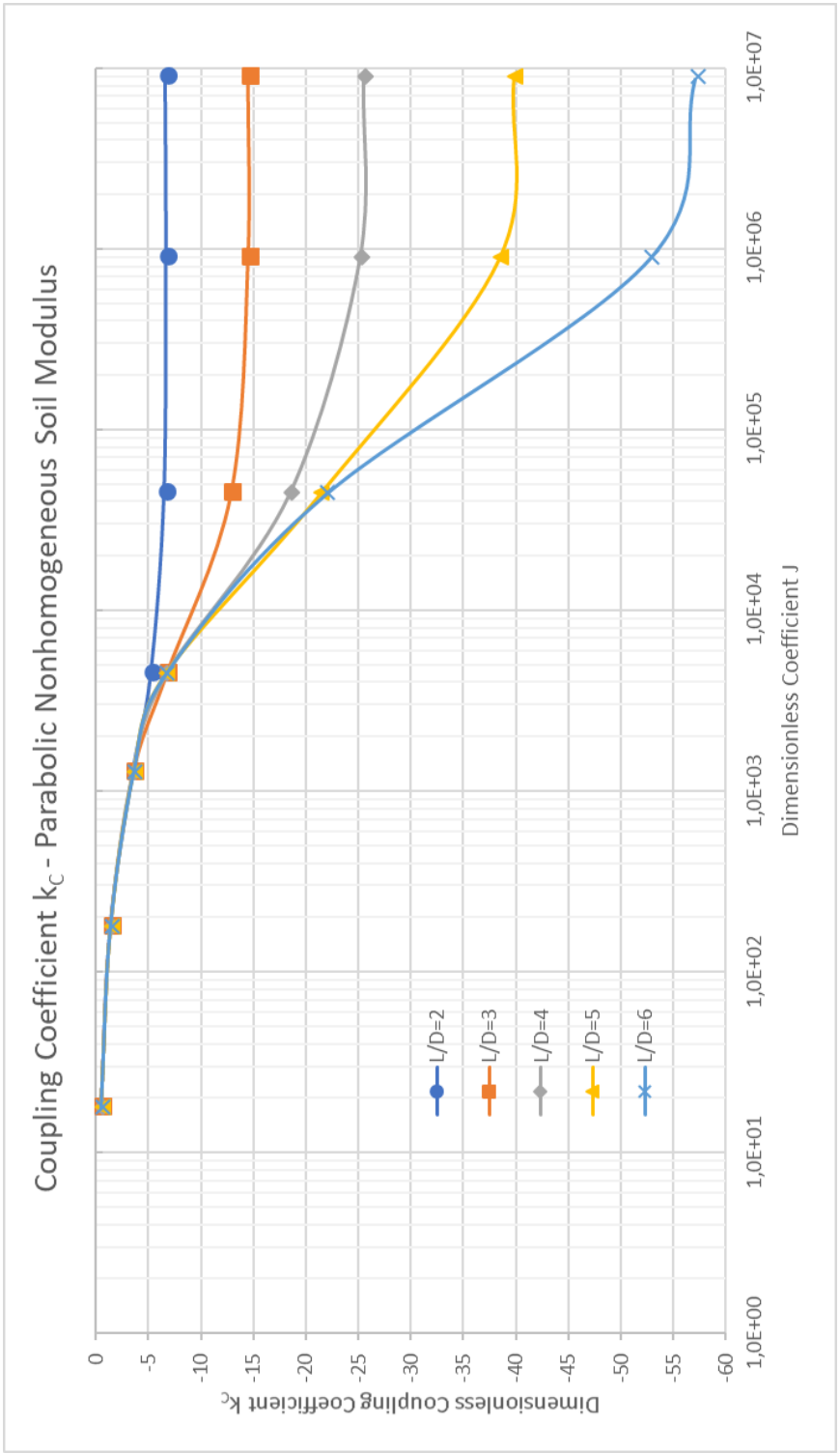

Figure 40: Normalized chart of the coupling stiffness in parabolic nonhomogeneous soil